Technical Report

海洋情報部研究報告 第 54 号 平成 29 年 3 月 27 日
REPORT OF HYDROGRAPHIC AND OCEANOGRAPHIC RESEARCHES No.54 March, 2017

Long-term stability of the kinematic Precise Point Positioning for the sea surface observation unit compared with the baseline analysis†

Shun-ichi WATANABE*1, *2, Yehuda BOCK*2, C. David CHADWELL*2,
Peng FANG*2, and Jianghui GENG*3

Abstract

Kinematic Precise Point Positioning (PPP) is an effective tool for tracking dynamic positions in the open ocean in support of GPS-A, because it does not require a local terrestrial reference site. In this study, we compared the solutions of the ship-borne 1 Hz GNSS data processed by different software to evaluate the long-term stability of the positioning. The results indicated that PPP solutions were more stable than the differential solutions, which were affected by the perturbation of the reference sites. We also found that the ambiguity-fixed PPP is capable of providing robust solutions, even in situations with loss of data.

1. Introduction

Precise kinematic positioning in the open ocean is a key component of seafloor geodetic observation using the GPS-Acoustic combined technique (GPS-A; e.g., Fujita et al., 2006). It requires the kinematic positioning of the sea-surface platform with an accuracy of a few centimeters to detect the seafloor displacement due to the plate motion and plate boundary deformation. In the Japan Coast Guard (JCG), the kinematic differential GNSS (Global Navigation Satellite System) software "Interferometric Translocation" (IT; e.g., Colombo, 1998) is used for the GPS-A routine analysis (Fujita et al., 2006). The accuracy and stability of IT had been discussed by several researchers in JCG (e.g., Fujita and Yabuki, 2003; Kawai et al., 2006; Saito et al., 2010). Kawai et al. (2006) showed that IT provided the stable results for the baseline range within 1000 km, which is a big advantage of IT for the use at the seismogenic zone along the major trenches. Meanwhile, the technique of Precise Point Positioning (PPP) is actually free from the limitation of distance. PPP is also useful when there is a need for precise dynamic position of the survey vessels in near real-time, because it does not require the transfer of additional high rate GNSS data at the terrestrial reference sites (more than 1 Hz) to the vessels. The reason for "near" real-time is due to the latency of collecting acoustic signals for the static seafloor positioning is longer than GNSS signal acquisition. It should be noted that high quality orbits and clocks should be available when using PPP.

† Received September 21, 2016; Accepted November 7, 2016
＊1 Ocean Research Laboratory, Technology Planning and International Affairs Division
＊2 Scripps Institution of Oceanography, University of California, San Diego
＊3 GNSS Research Center, Wuhan University

Geng et al. (2010) reported that their PPP results for the vessel sailing in the Bohai Sea achieved a horizontal accuracy of 1 cm when using a reference network with an extent of a few thousand kilometers. If its accuracy is stably achieved in the Pacific, PPP would be an alternative way to determine the vessel's position. In this study, we evaluate the accuracy and stability of kinematic PPP results processed by several software, using the actual GNSS data collected for the GPS-A observation.

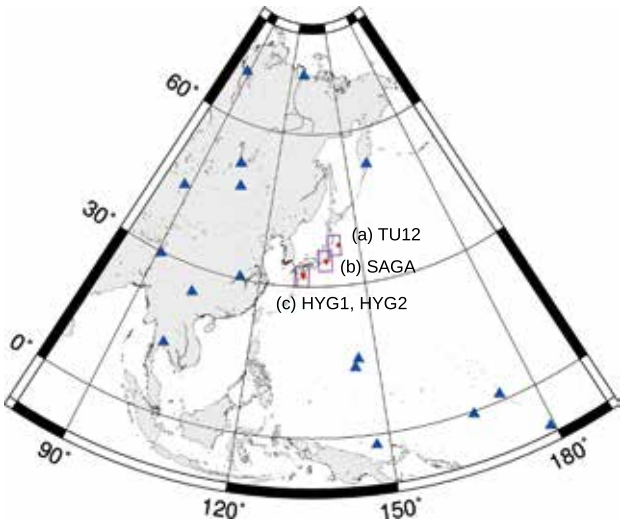

Fig. 1. Locations of the GPS-A sites where the rover's data in this study were collected (red circles). Blue triangles indicate the locations of the IGS stations used for the network solution in PANDA. Purple rectangular areas are enlarged in Fig. 2.

図 1. 測量船の観測データが取得された GPS-A 観測点の位置（赤丸）．PANDA のネットワーク解で使用した IGS 観測点位置を青三角で示す．紫で囲まれた領域は図 2 で拡大表示される領域を示す．

2. Data and Methods

The ship-borne 2 Hz GNSS data (dual frequency) were collected on the mast of the JCG survey vessels for the GPS-A observation as the rover station (Table 1a). We reduced the rover's GNSS data to 1 Hz, in order to compare them with the 1 Hz terrestrial GNSS sites (used as the reference sites for the baseline analysis) at the same sampling rate. The locations of the GPS-A sites (i.e., approximate area of the rover's track) are shown in Figs. 1 and 2. The rover's GNSS data

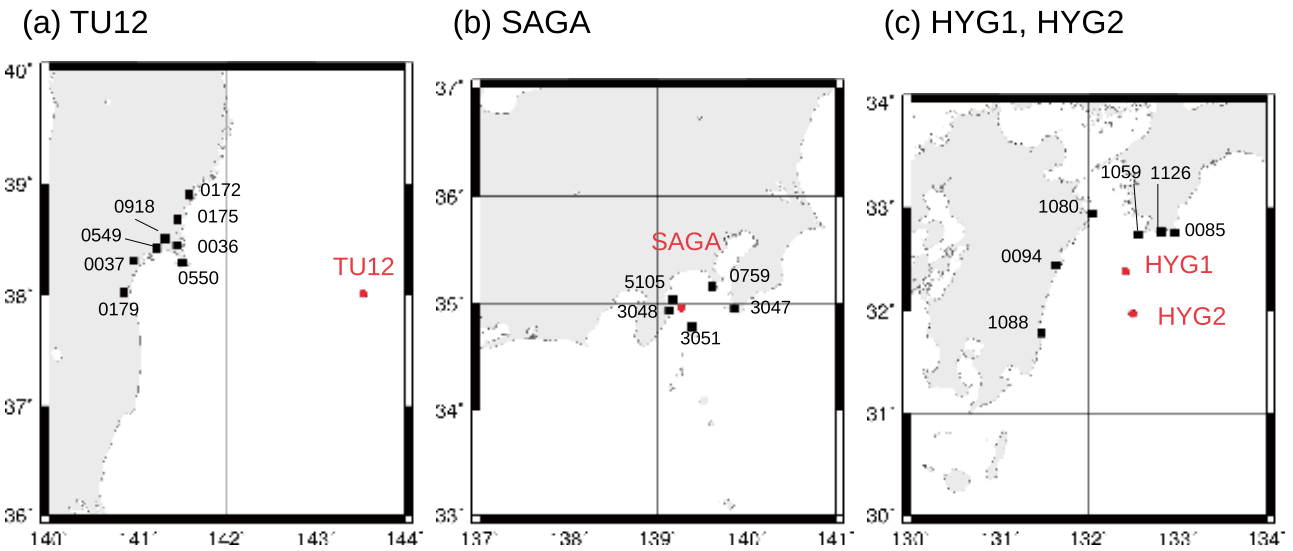

Fig. 2. Locations of the GPS-A sites where the rover's data in this study were collected (red circles) and the terrestrial reference sites for the differential positioning in IT (black squares) for (a) TU12, (b) SAGA, and (c) HYG1 and HYG2.

図 2. 測量船の観測データが取得された GPS-A 観測点（赤丸）および IT の基線解析で使用した陸上固定観測点（黒四角）の位置．(a) TU12, (b) SAGA, (c) HYG1 および HYG2 についてそれぞれ示す．

Table 1. Specifications of the GNSS data.
表 1. GNSS データの諸元.

(a) GPS-A site

GPS-A site	TU12	SAGA	HYG1	HYG2
Center position for local coordinates	38.02 °N 143.53 °E	34.96 °N 139.26 °E	32.38 °N 132.42 °E	31.97 °N 132.49 °E
Data period [UTC]	(1) 2015/04/27 0500 - 2015/04/27 2359 (2) 2015/08/07 1200 - 2015/08/08 1159 (3) 2015/10/23 0100 - 2015/10/23 2232	(1) 2012/11/24 0200 - 2012/11/24 2159	(1) 2015/05/29 2000 - 2015/05/30 1124 (2) 2015/09/11 1200 - 2015/09/12 0400 (3) 2015/12/12 0100 - 2015/12/12 0950 (4) 2016/01/16 1000 - 2016/01/17 0112 (5) 2016/03/19 2300 - 2016/03/20 1505	(1) 2015/05/28 1800 - 2015/05/29 0240 (2) 2015/05/29 1000 - 2015/05/29 2025 (3) 2015/09/12 0400 - 2015/09/12 2359 (4) 2016/01/15 1500 - 2016/01/16 0837
Satellite	GPS	GPS	GPS	GPS
Reference site for IT (Approx. range)	0036 (190 km) 0037 (230 km) 0172 (200 km) 0175 (200 km) 0179 (240 km) 0549 (210 km) 0550 (180 km) 0918 (200 km)	0759 (40 km) 3047 (50 km) 3048 (10 km) 3051 (20 km) 5105 (10 km)	0085 (70 km) 0094 (70 km) 1059 (40 km) 1080 (70 km) 1088 (110 km) 1126 (60 km)	0085 (100 km) 0094 (100 km) 1059 (90 km) 1080 (120 km) 1088 (100 km) 1126 (90 km)

(b) SIO buoy

Rover name	SIO buoy
Center position for local coordinates	33.21 °N 118.39 °W
Data period [UTC]	2011/03/14 0000 - 2011/03/14 2359 (no data between 0600-0700)
Satellite	GPS

Table 2. Configurations for each positioning method.
表 2. 各 GNSS 解析手法の設定.

Software	Mode	Orbit	Clock	FCB	Reference site	Coordinates
PANDA	PPP-AR	IGS Final	Estimate (30 sec)	Estimate	N/A	ITRF2008
RTKLIB	PPP	IGS Final	IGS Final (30 sec)	N/A	N/A	ITRF2008
IT	Differential	IGS Final	N/A	N/A	GEONET station	GEONET F3 (ITRF2005)

were processed by the following PPP software; PANDA (developed in Wuhan University; Shi et al., 2008) and RTKLIB ver. 2.4.2 (open source package developed by Dr. Takasu; available at http://www.rtklib.com/).

PANDA is the software used in the Scripps Orbit and Permanent Array Center (SOPAC). It has been modified at SOPAC for real-time earthquake and tsunami warning systems (Geng et al., 2013; Melgar and Bock, 2015). The satellite clock and the fractional cycle bias (FCB) were estimated using the regional GNSS network by PANDA, which enables us to fix ambiguities for kinematic PPP (Ge et al., 2008; Geng et al., 2009). Geng et al. (2010) had studied the dependency of the accuracy on the scale of the reference network, and suggested that an accuracy of several centimeters requires the network width of up to a few thousands kilometers. However, because the IGS (International GNSS Service) stations around Japan are largely affected by the co- and post-seismic deformation associated with the 2011 Tohoku-oki earthquake (M 9.0), we selected the IGS stations in broader area for the network solution (Fig. 1). Another software, RTKLIB, has the GUI (graphical user interface) mode for Windows OS, which is an advantage for users who are unfamiliar with the CUI (character user interface) to learn and use rather than other software. We also processed the rover's data by RTKLIB in PPP mode to compare the results. We used the IGS final product for the satellite clock data with the interval of 30 sec for RTKLIB (ftp://igscb.jpl.nasa.gov/igscb/product/).

To compare the results by PPP with the differential positioning, we determined the rover's position using IT ver. 4.2 in differential mode. The 1 Hz GNSS data collected at the GEONET stations by the Geospatial Information Authority of Japan (GSI) were used as the reference sites (Table 1a, Fig. 2). We fixed their positions to the daily F3 position (Nakagawa et al., 2009), taking the 7-day average after removing the 2-sigma outliers. We used the satellite orbits and the earth rotation parameters from the IGS final products (ftp://igscb.jpl.nasa.gov/igscb/product/) for all analysis. Configurations for three methods are summarized in Table 2.

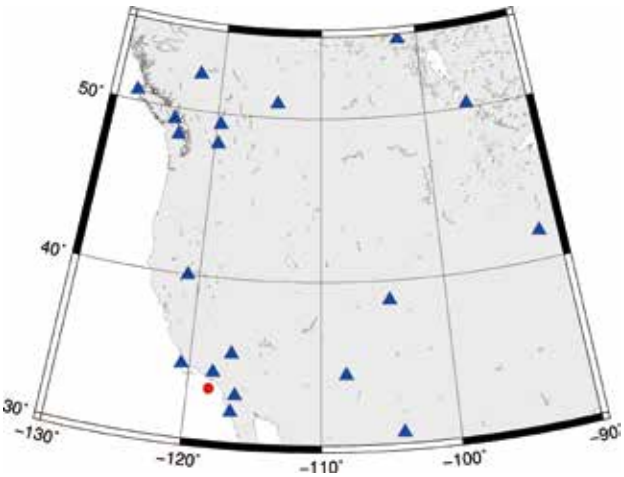

Fig. 3. Location of the SIO buoy where the GNSS data was collected (red circle). Blue triangles indicate the locations of the IGS stations used for the network solution in PANDA.

図 3. SIO ブイの GNSS データが取得された海域(赤丸). PANDA のネットワーク解で使用した IGS 観測点位置を青三角で示す.

In addition to the GNSS data in Japan, we processed the data in the western off the Pacific coast of southern California, U.S., using PANDA and RTKLIB (Table 1b, Fig. 3), which had been collected on the buoy operated by Dr. C. D. Chadwell of the Scripps Institution of Oceanography (hereafter called SIO buoy data). We then compared the results with the ambiguity-fixed PPP solution using GIPSY software (Bertiger et al., 2010), which is developed by the Jet Propulsion Laboratory, NASA (https://gipsy-oasis.jpl.nasa.gov/). The IGS stations used for the reference network in PANDA are shown in Fig. 3.

3. Results

The position differences for the JCG's GNSS data in the local ENU coordinates between (i) PANDA and RTKLIB, and (ii) PANDA and IT are shown in Figs. 4 and 5, respectively. The positions of the reference sites used in IT were also solved by PANDA as the pseudo-kinematic rover station (displayed as green lines in Fig. 5). The averages and standard deviations of the position difference are shown in Table 3.

Fig. 4 and Table 3 indicate that PANDA and RTKLIB provided the consistent results within a few centimeters for the horizontal component. Standard deviations of horizontal discrepancy were less than 2 cm, except the campaign on 2015/09/12 at HYG2 where the difference was increased at the end of the session. On the other hand, standard deviations of vertical discrepancies were up to 10 cm. As shown in the time series (Fig. 4), the vertical discrepancies in some campaigns steeply increased with more than 20 cm for 10–30 minutes. It caused the larger standard deviations in the vertical component.

The results by IT had biases of several centimeters from the PPP results. As shown in Fig. 5, the long-term variations including the offset of the position difference were similar to those of the reference sites. Their standard deviations were the same as those of differences between PANDA and RTKLIB within 1–2 cm, except several cases such as the campaign on 2015/04/27 at TU12 with the reference site 0175. Because the other baseline

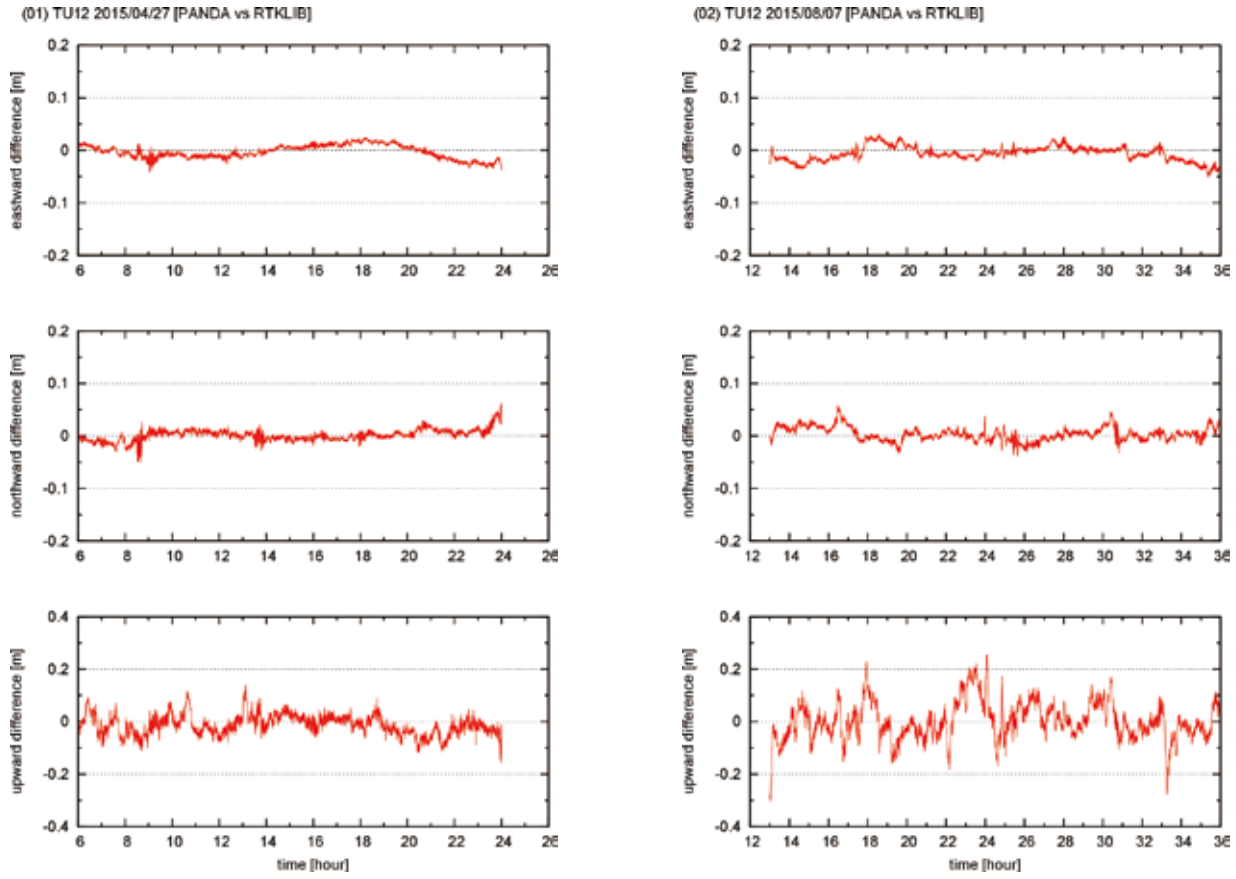

Fig. 4. Time series of position differences between the results by PANDA and RTKLIB for each campaign in the local ENU coordinates. The eastern, northern, and vertical components are displayed on the top, middle, and bottom panels, respectively.

図 4. PANDA と RTKLIB で得られた，各キャンペーン（01）–（13）における測量船位置解の偏差の時系列．偏差はローカル ENU 座標系を用いて，上からそれぞれ東向き，北向き，上向きの成分を示す．

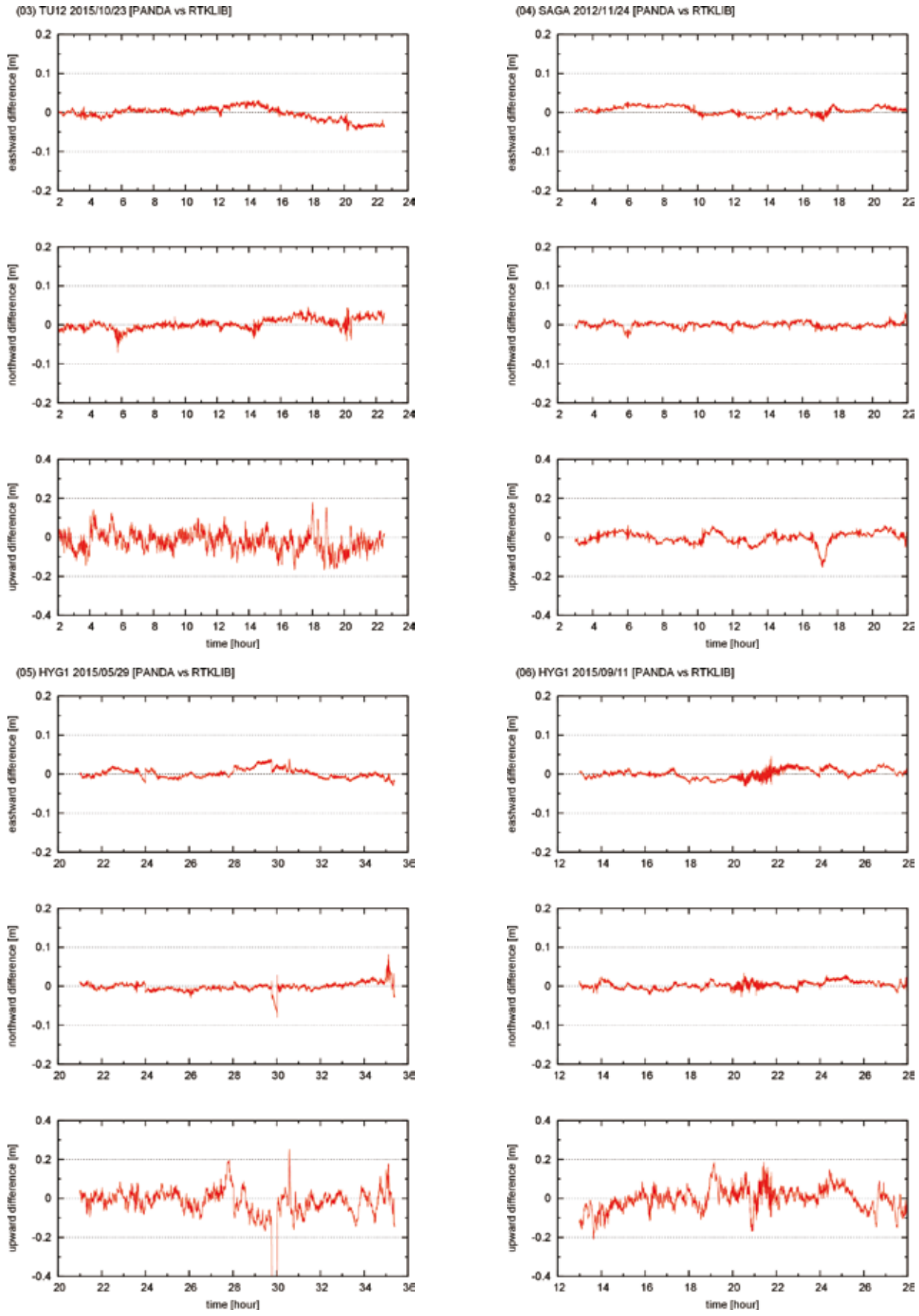

Fig. 4. （continued）
図 4.（続き）

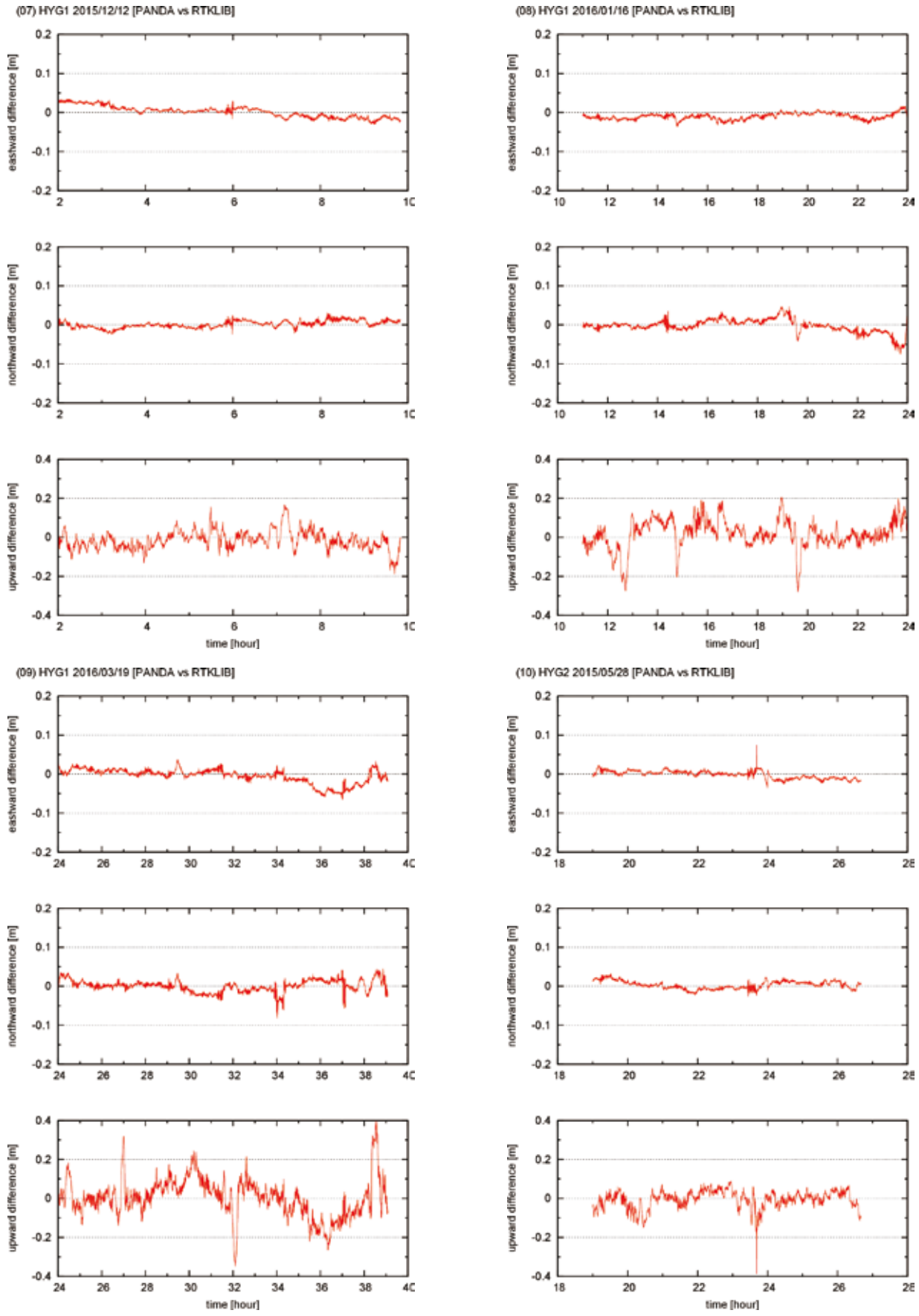

Fig. 4. （continued）
図 4.（続き）

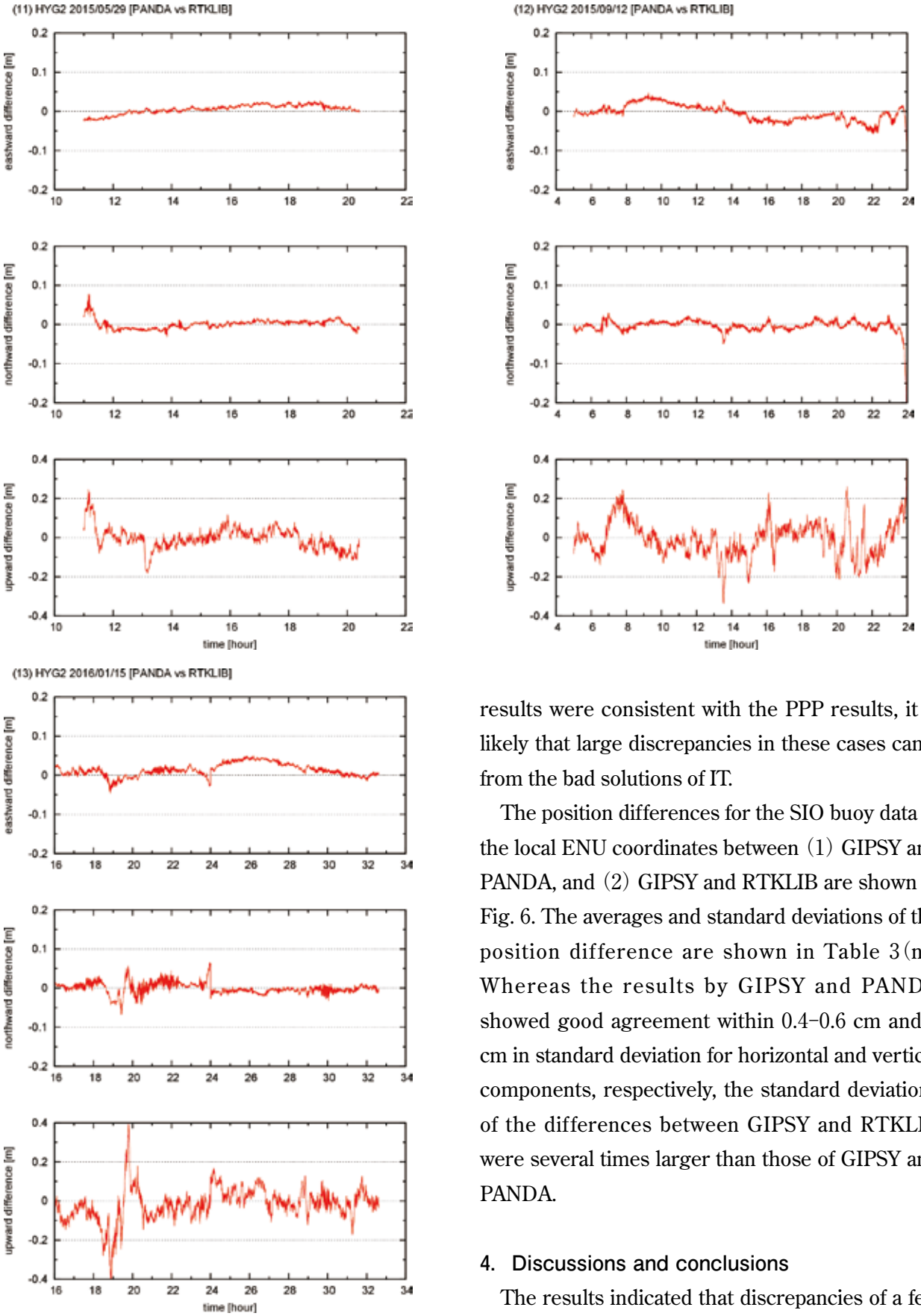

Fig. 4. （continued）
図 4.（続き）

results were consistent with the PPP results, it is likely that large discrepancies in these cases came from the bad solutions of IT.

The position differences for the SIO buoy data in the local ENU coordinates between (1) GIPSY and PANDA, and (2) GIPSY and RTKLIB are shown in Fig. 6. The averages and standard deviations of the position difference are shown in Table 3(n). Whereas the results by GIPSY and PANDA showed good agreement within 0.4–0.6 cm and 2 cm in standard deviation for horizontal and vertical components, respectively, the standard deviations of the differences between GIPSY and RTKLIB were several times larger than those of GIPSY and PANDA.

4. Discussions and conclusions

The results indicated that discrepancies of a few centimeters in standard deviation were found between the three different GNSS software. In

some cases of the IT solution, the selection of the reference site would largely affect the rover's positioning. To avoid such outliers, one can choose better solutions by comparing the IT results with several different references. Actually, the IT solutions are compared with the sea surface height model, with the assumption that the vessels are constrained on the sea surface (Fujita and Yabuki, 2003).

In the case of the SIO buoy, the lack of data between 6:00 and 7:00 (UTC) was considered to cause the step-wise discrepancy between GIPSY and RTKLIB, especially in eastern component. Although it seemed to be restored at 10:20–10:30 (UTC), this was likely caused by other reason. Because we set RTKLIB to remove the GNSS data during the eclipse, only 4 satellites were available during 10:20–10:25 (UTC), which might cause another step-wise offset. In addition, less than 4 satellites were available at 20:41, when spiky noises appeared in both results in Fig. 6. However, the missing would not affect to the difference between GIPSY and PANDA. These facts indicated that GIPSY and PANDA provide the similar and robust PPP solutions for the missing data, though it does not necessarily mean the more accurate solutions.

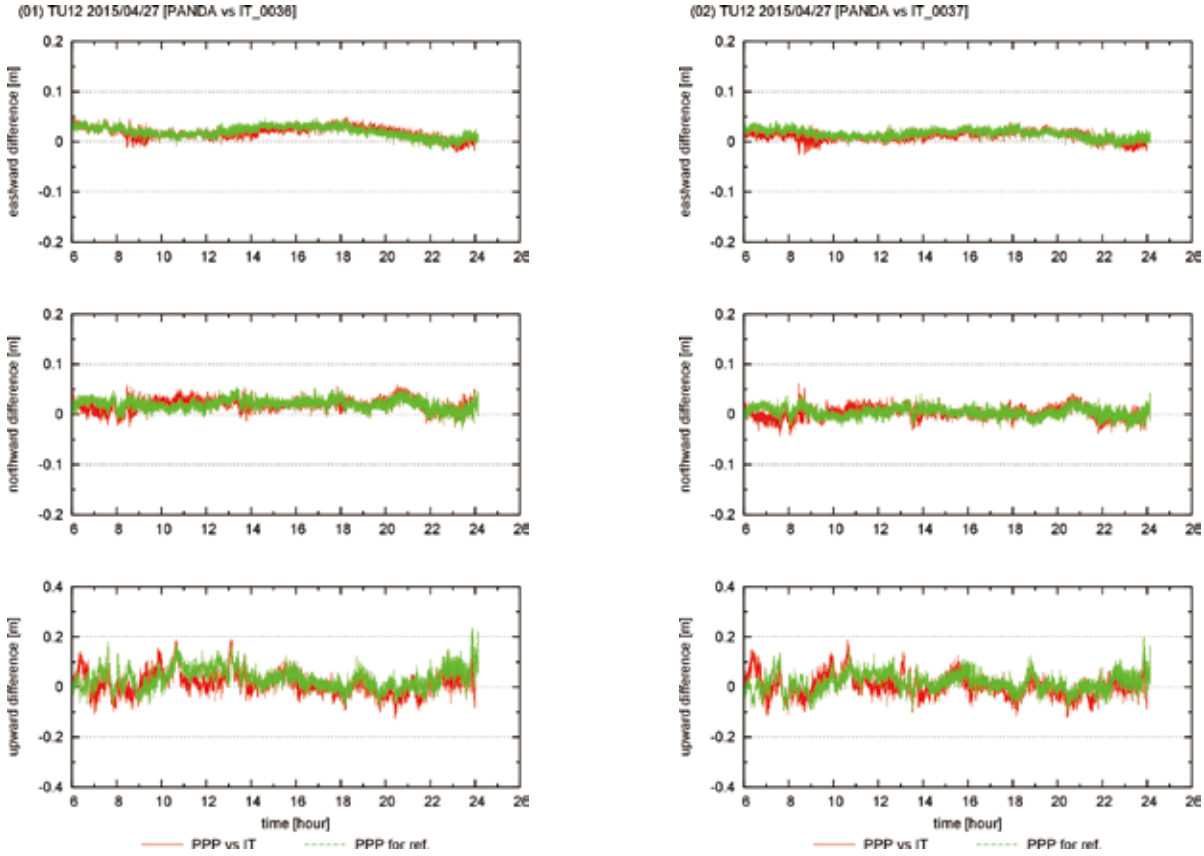

Fig. 5. Time series of position differences between the results by PANDA and IT for each campaign and each reference site in the local ENU coordinates (red lines). The names of the reference site for IT are shown on the title as IT_[site name]. The eastern, northern, and vertical components are displayed on the top, middle, and bottom panels, respectively. Green lines indicate the pseudo-kinematic solution of the reference site solved by PANDA, relative to the fixed position used in IT.

図 5. PANDA と IT で得られた，各キャンペーン及び各基線 (01) – (82) における測量船位置解の偏差の時系列 (赤線)．偏差はローカル ENU 座標系を用いて，上からそれぞれ東向き，北向き，上向きの成分を示す．IT で使用した固定局は各グラフのタイトルに示されている．緑線は，各固定局の位置を移動局として PANDA で解いた際の位置時系列を，IT における固定座標からの偏差として示した時系列である．

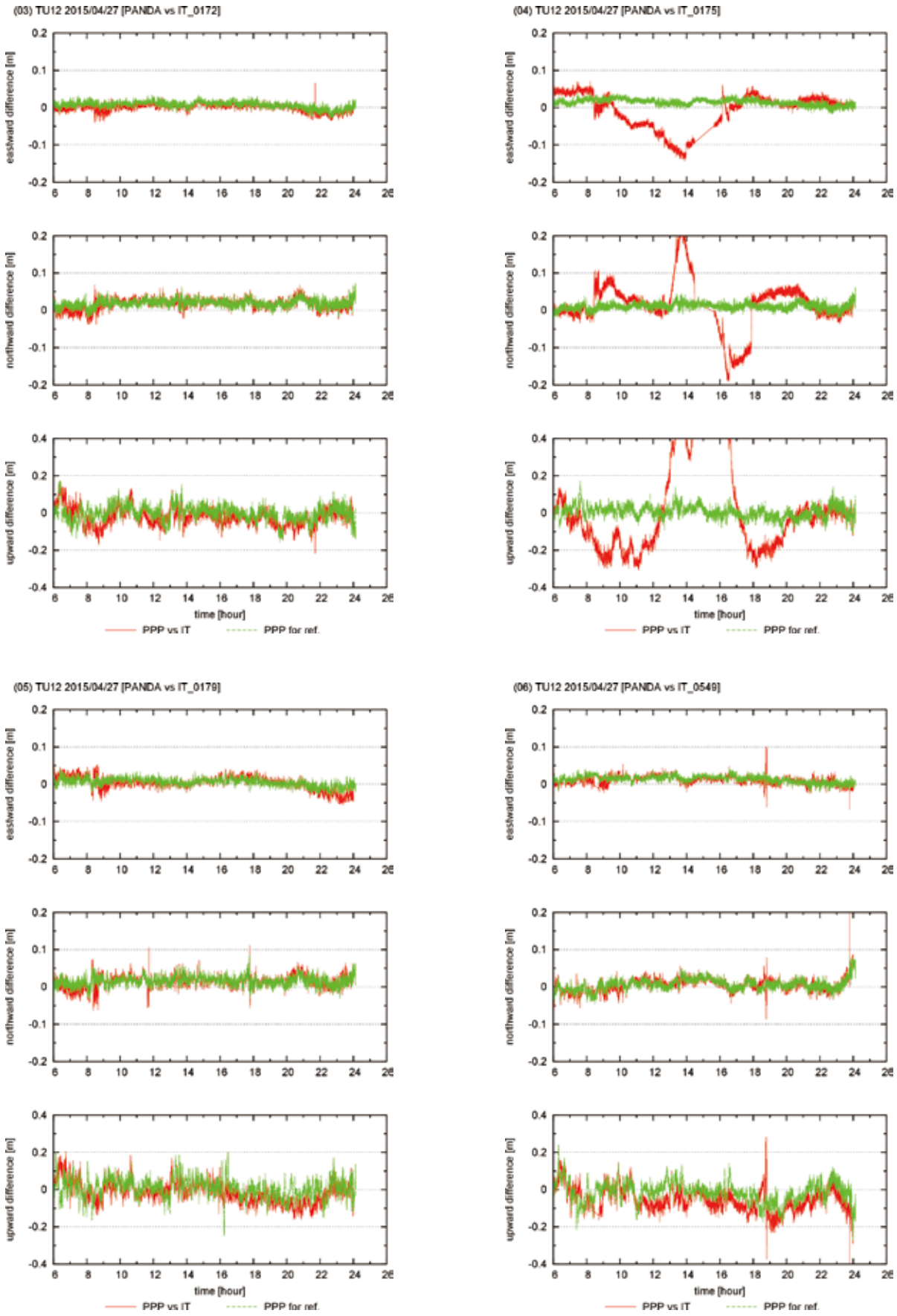

Fig. 5. （continued）
図 5.（続き）

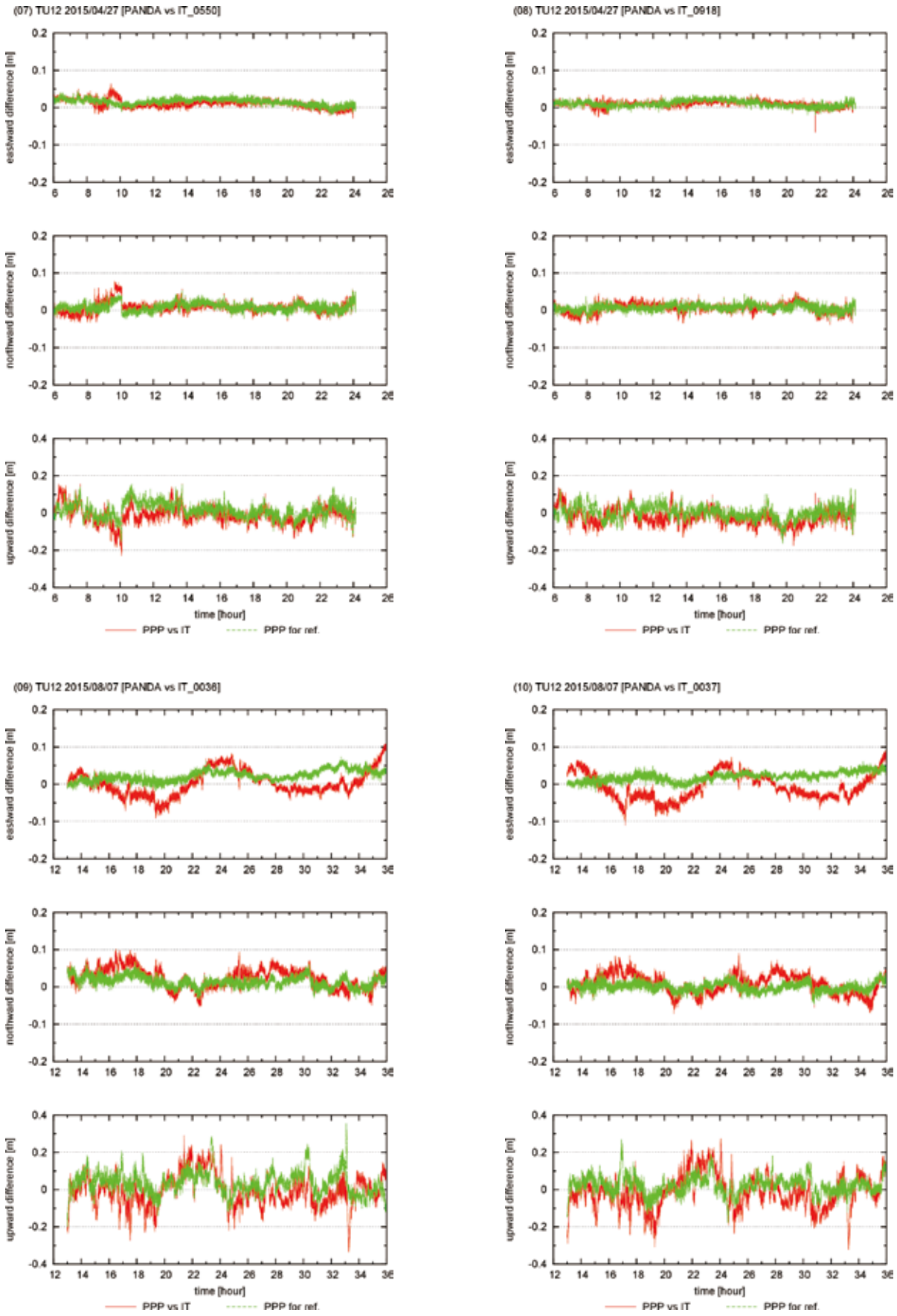

Fig. 5. （continued）
図 5.（続き）

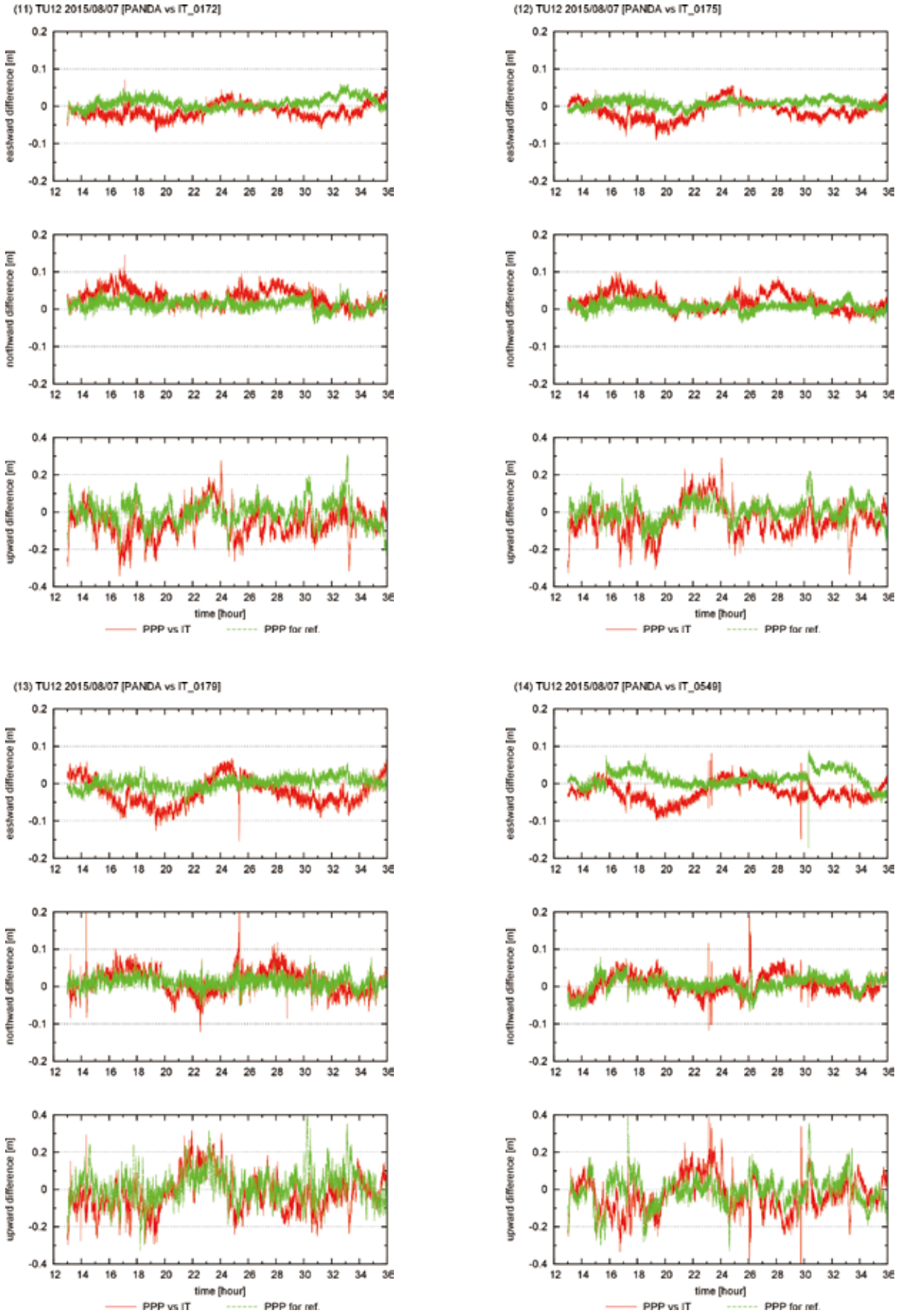

Fig. 5. （continued）
図 5.（続き）

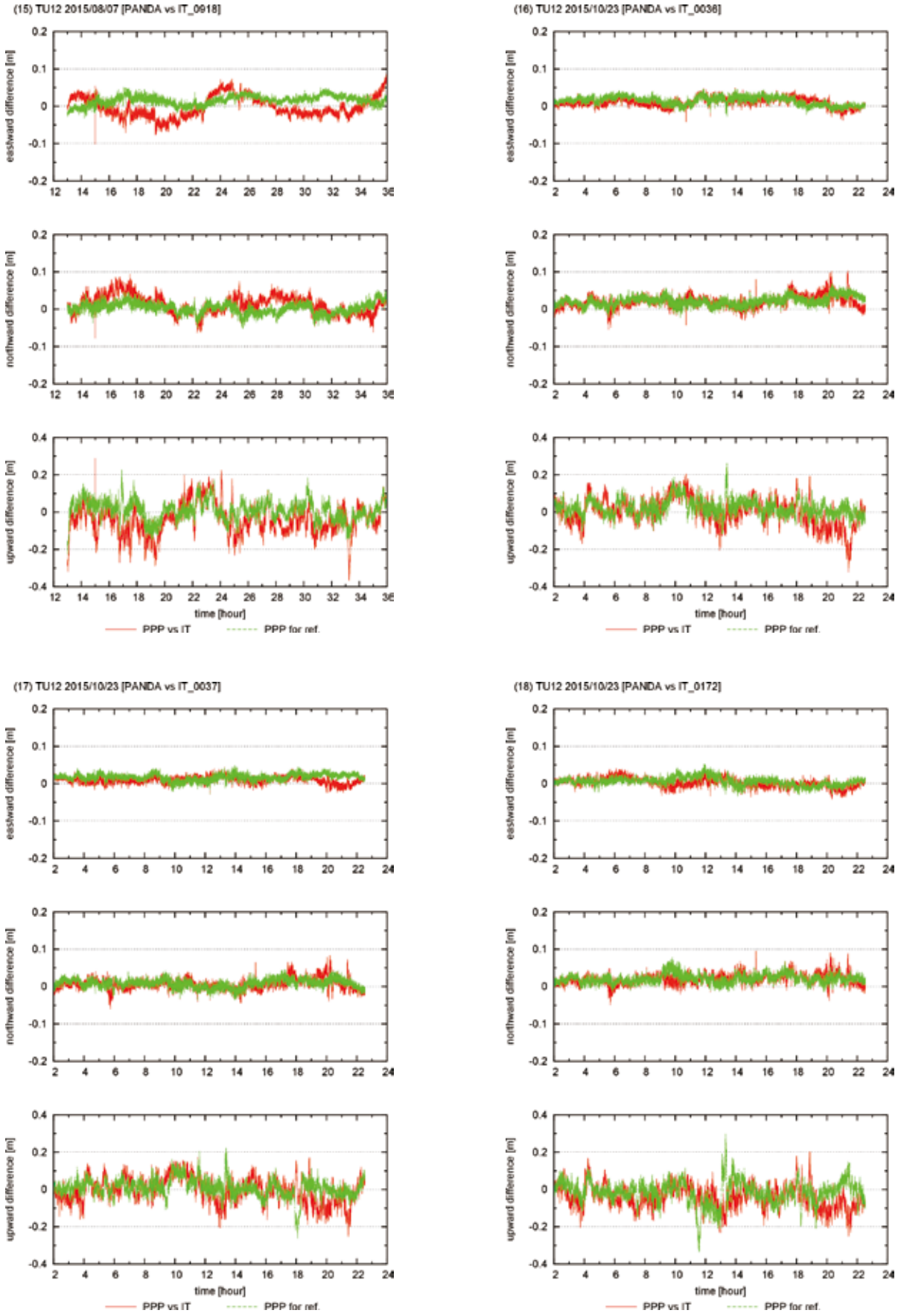

Fig. 5. （continued）
図 5.（続き）

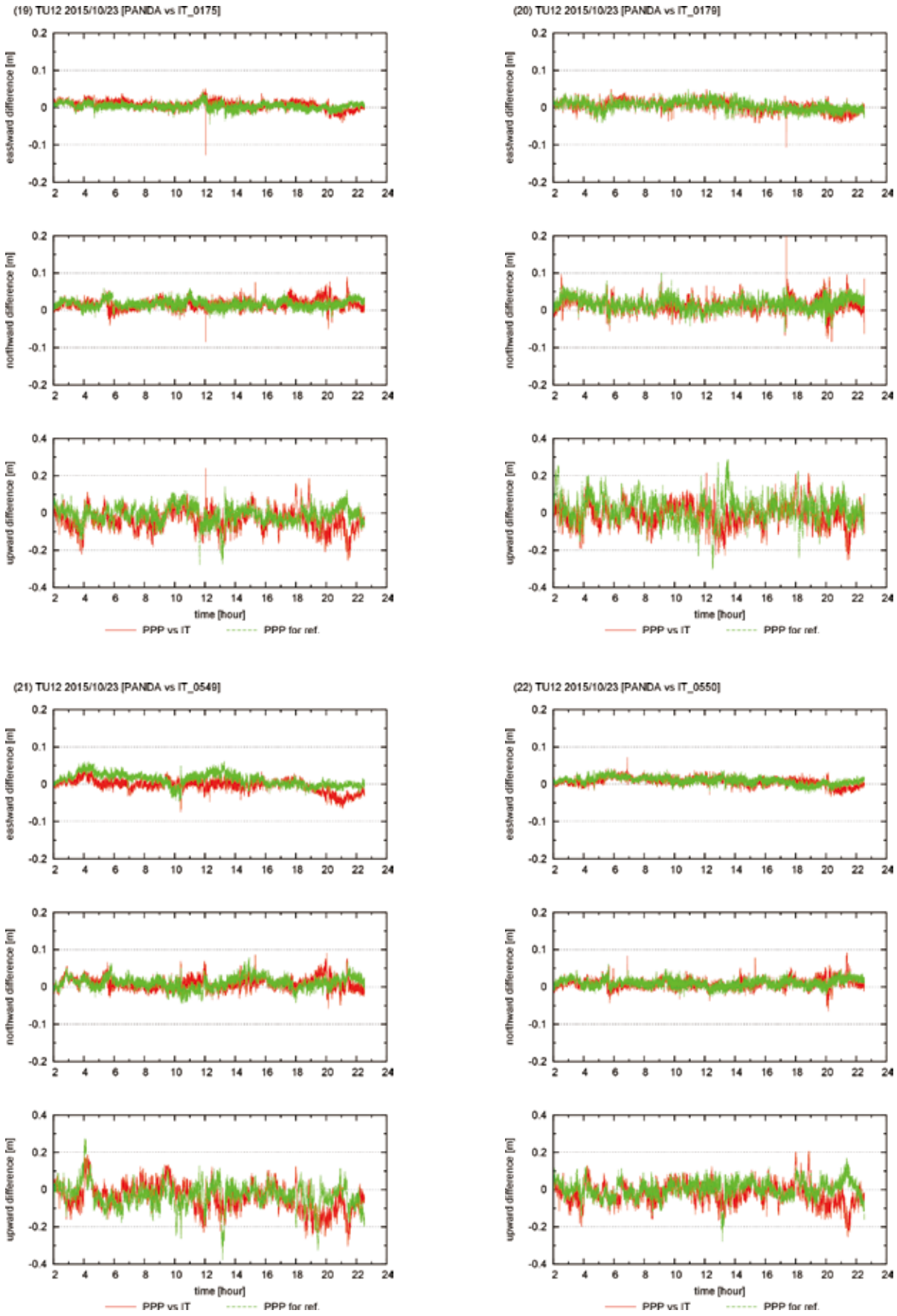

Fig. 5. （continued）
図 5.（続き）

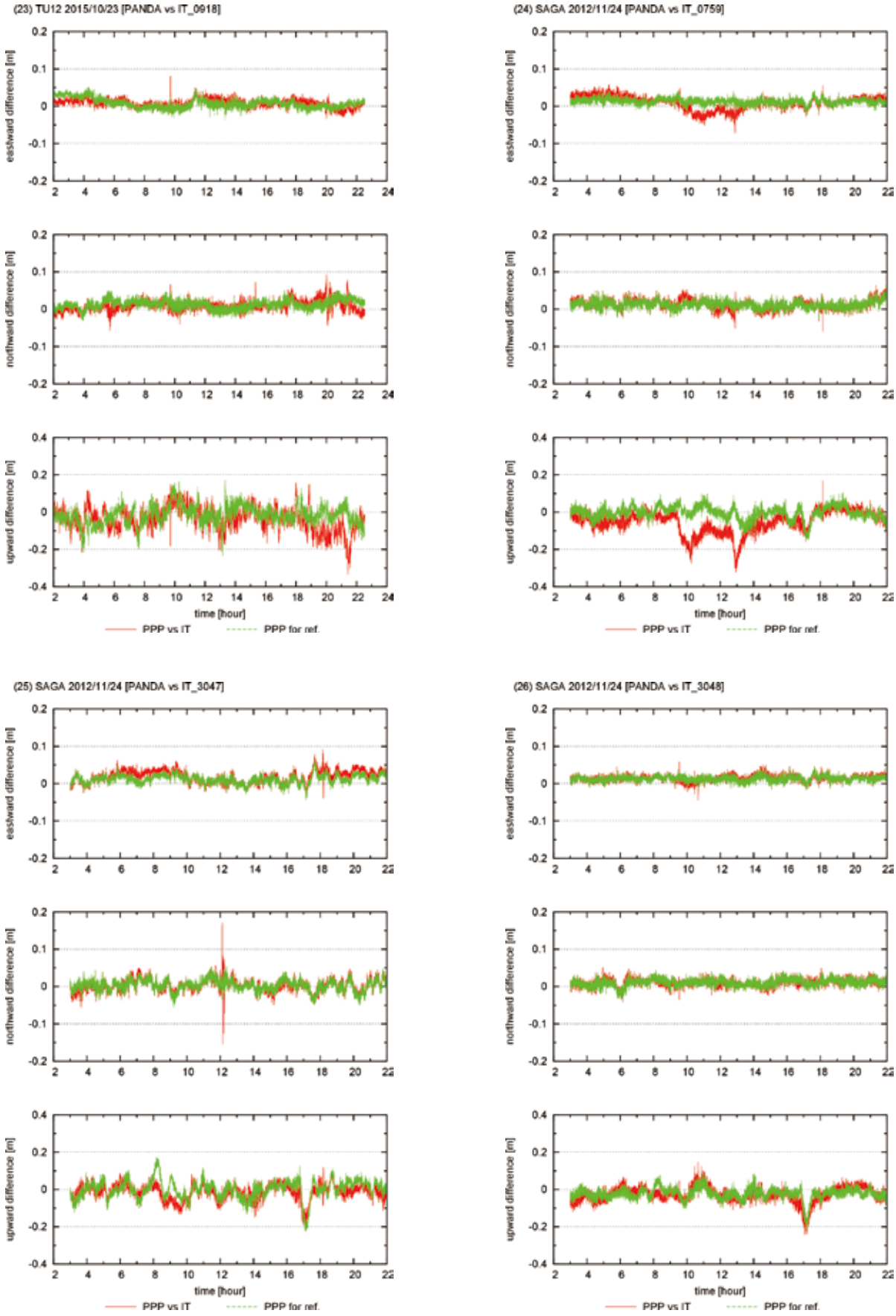

Fig. 5. （continued）
図 5.（続き）

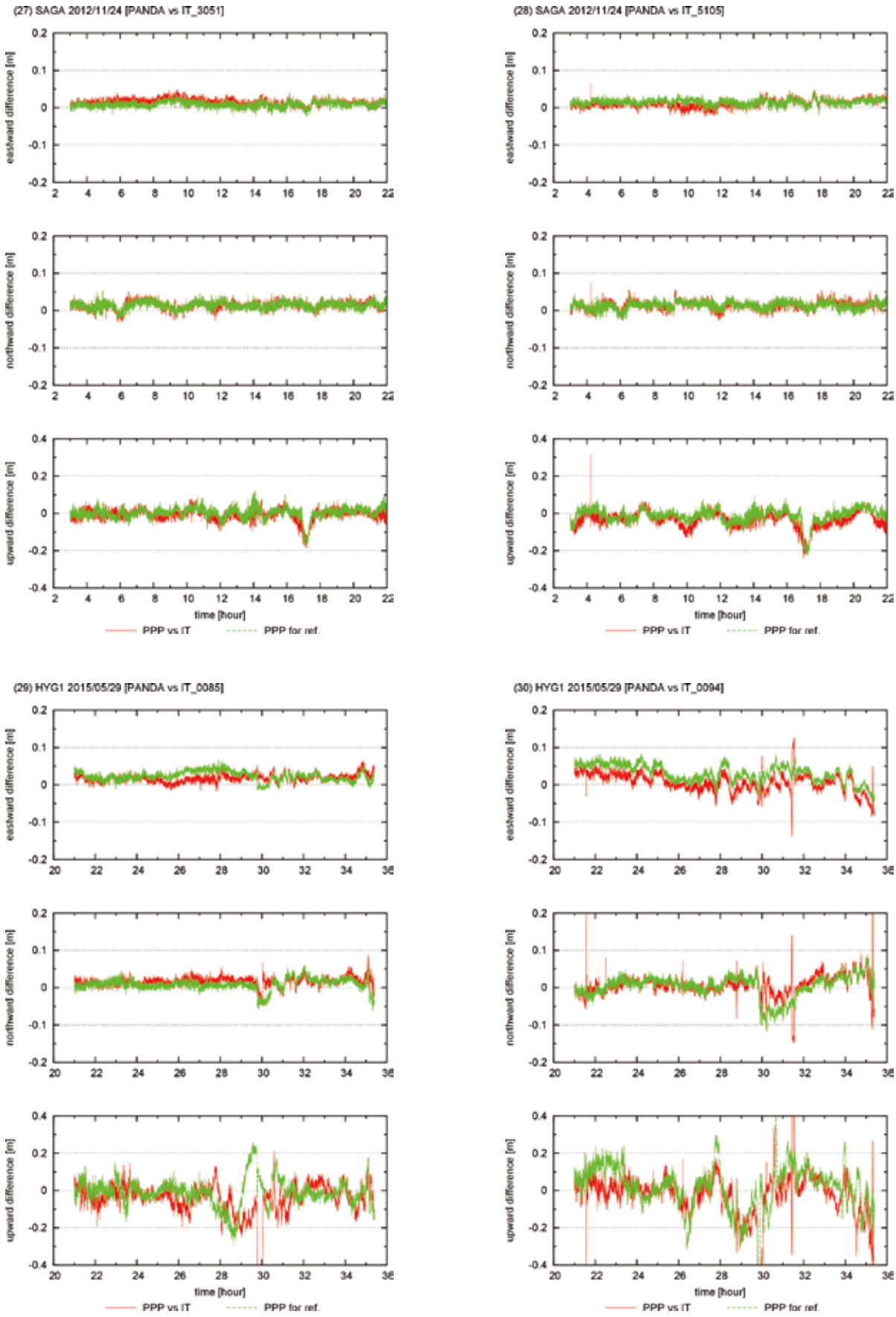

Fig. 5. （continued）
図 5.（続き）

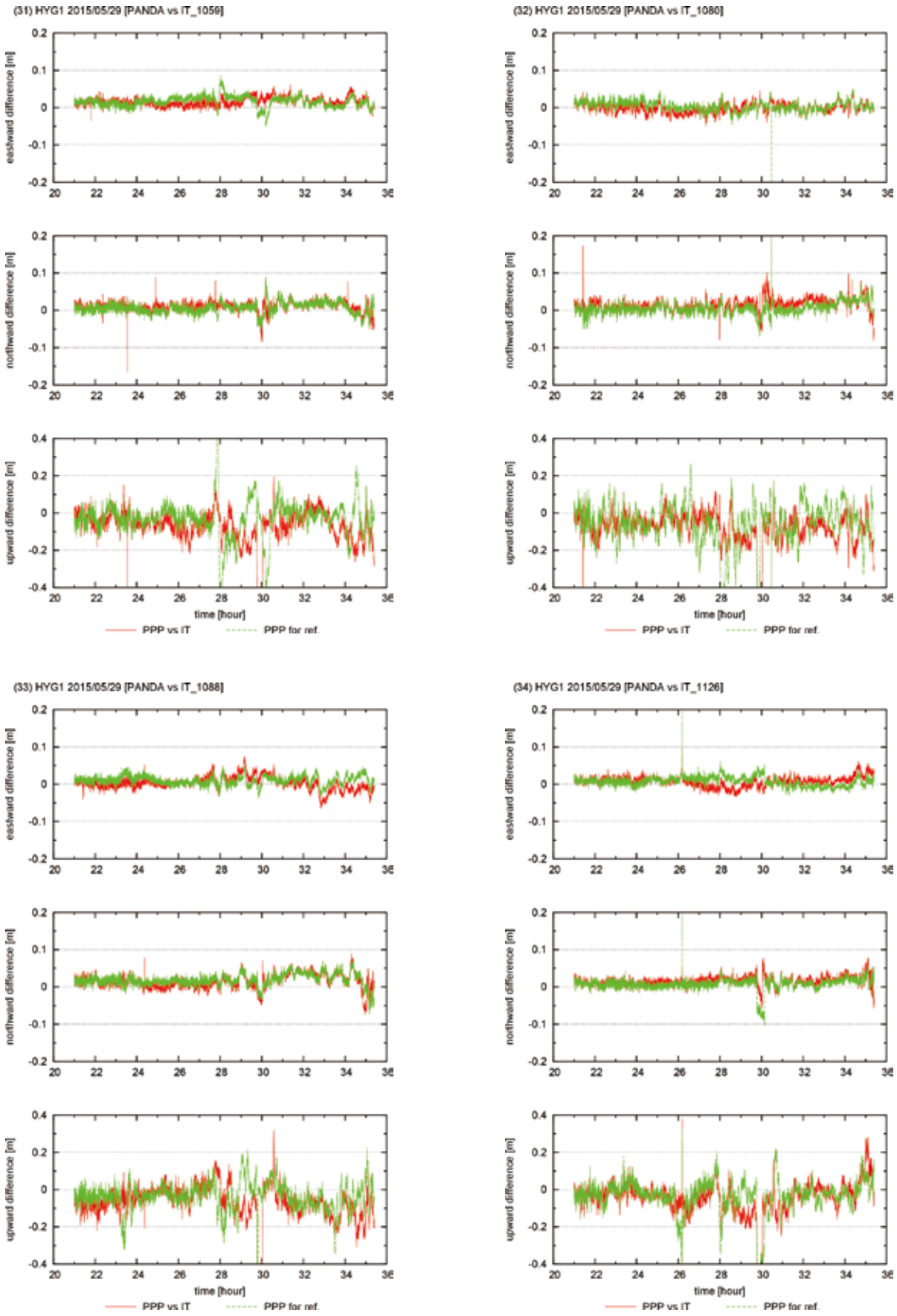

Fig. 5. （continued）
図 5.（続き）

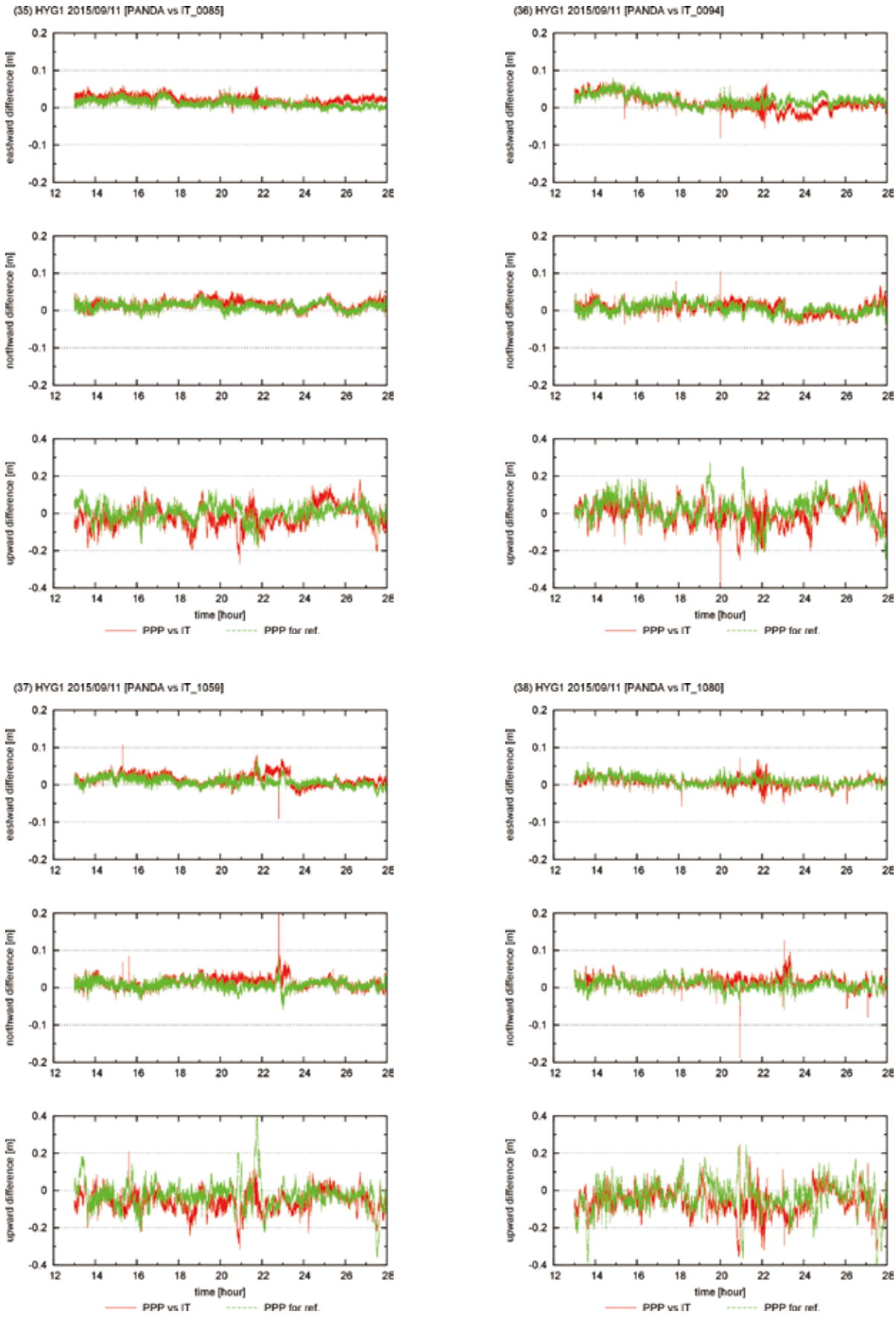

Fig. 5. （continued）
図 5.（続き）

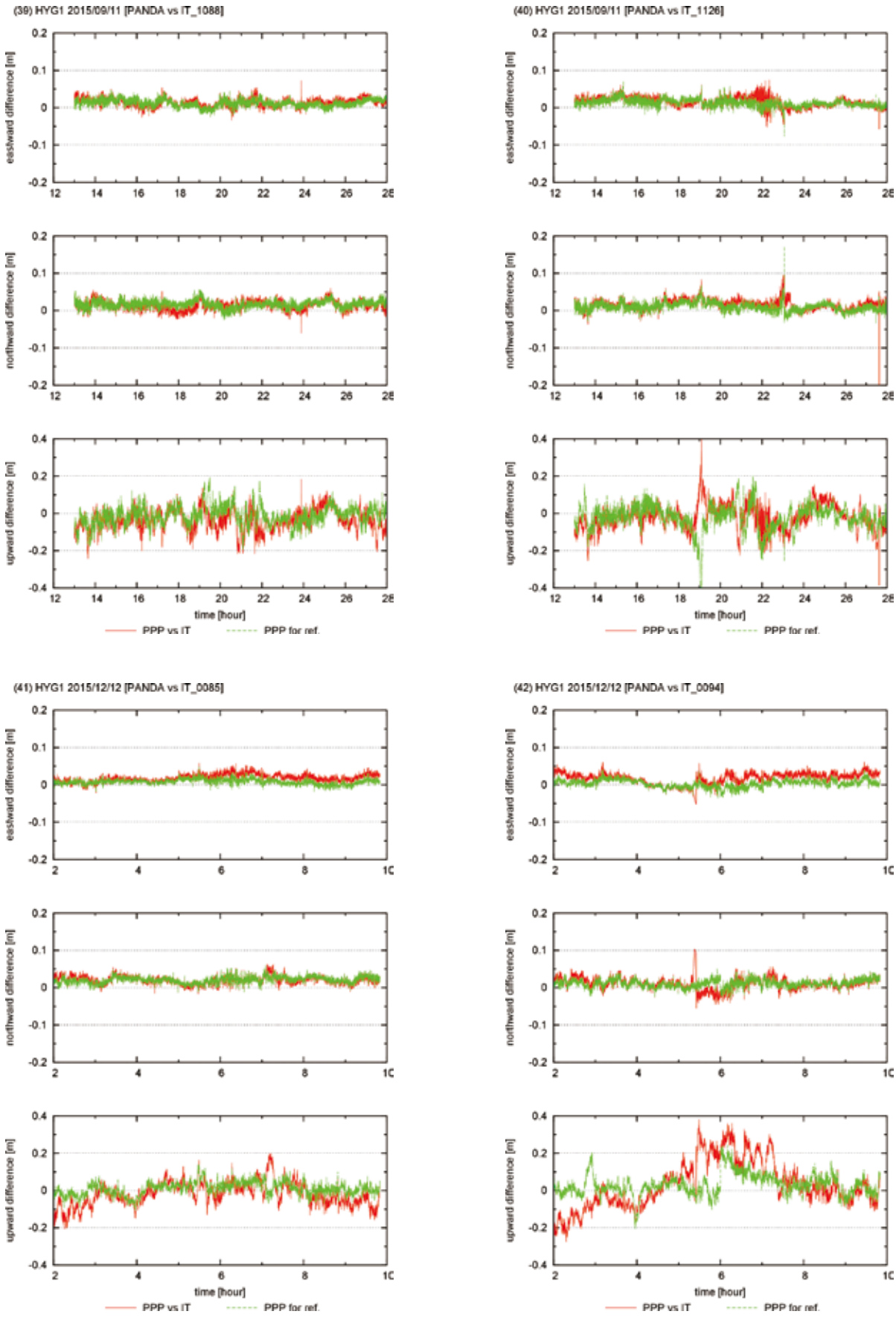

Fig. 5. （continued）
図 5.（続き）

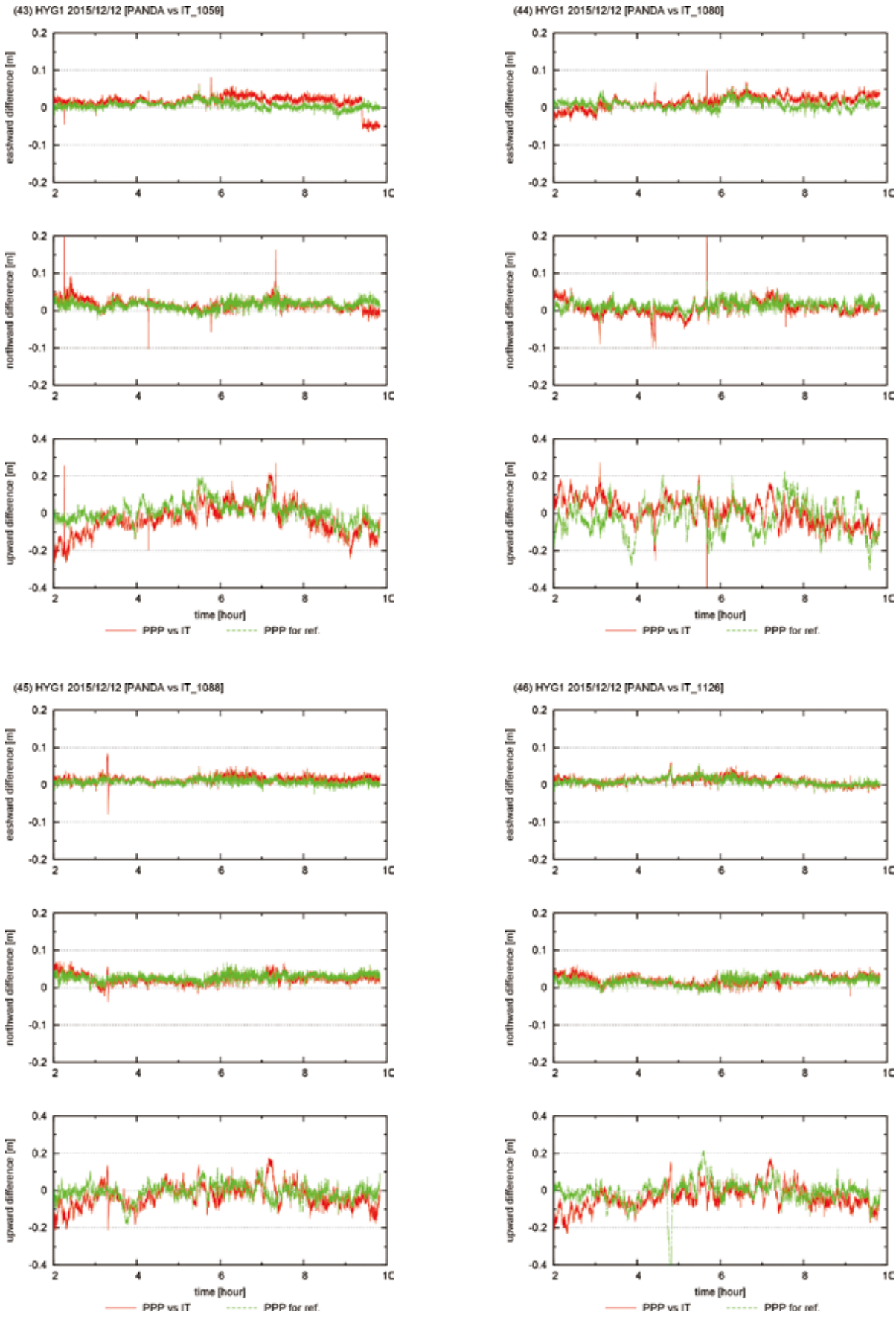

Fig. 5. （continued）
図 5.（続き）

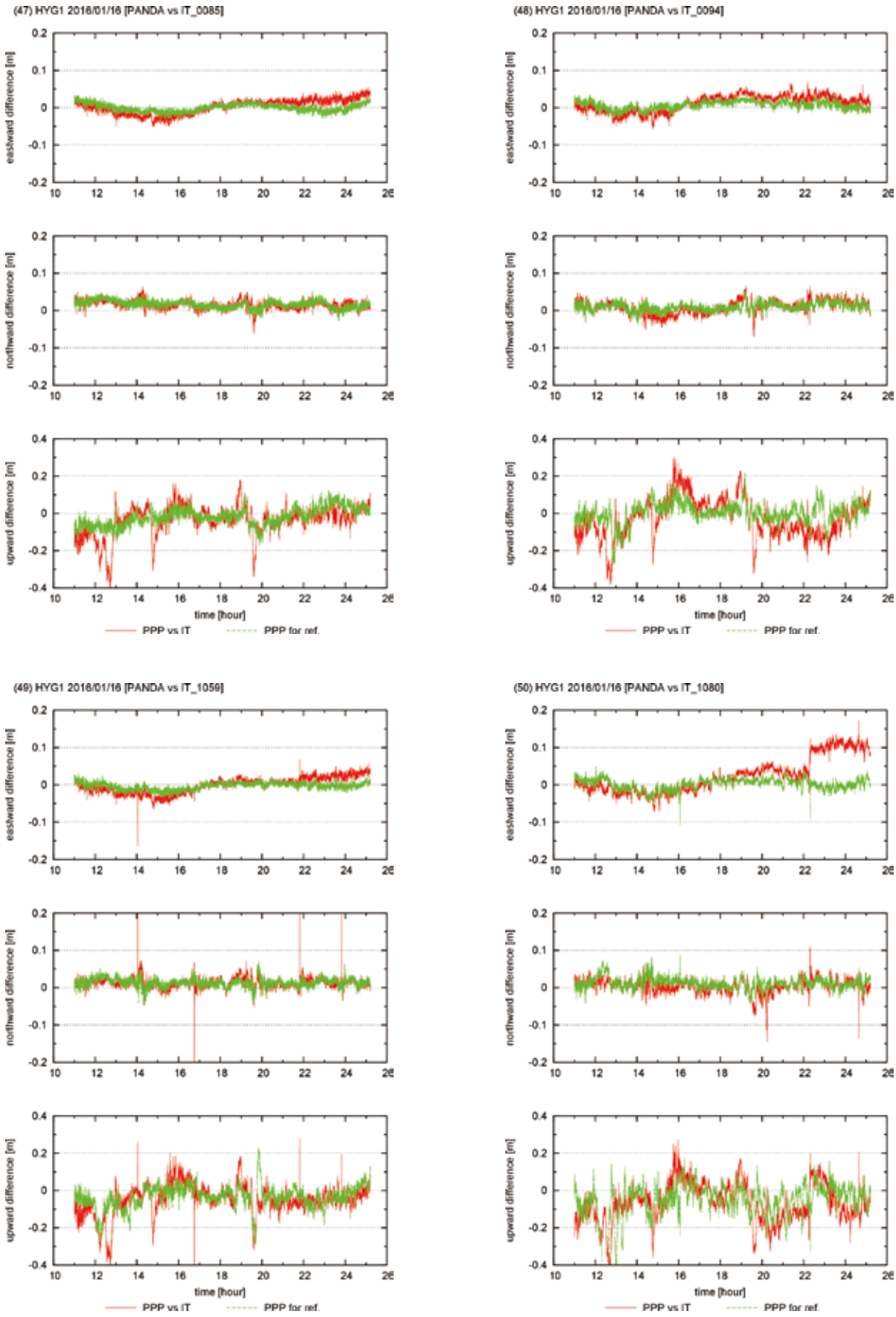

Fig. 5. （continued）
図 5.（続き）

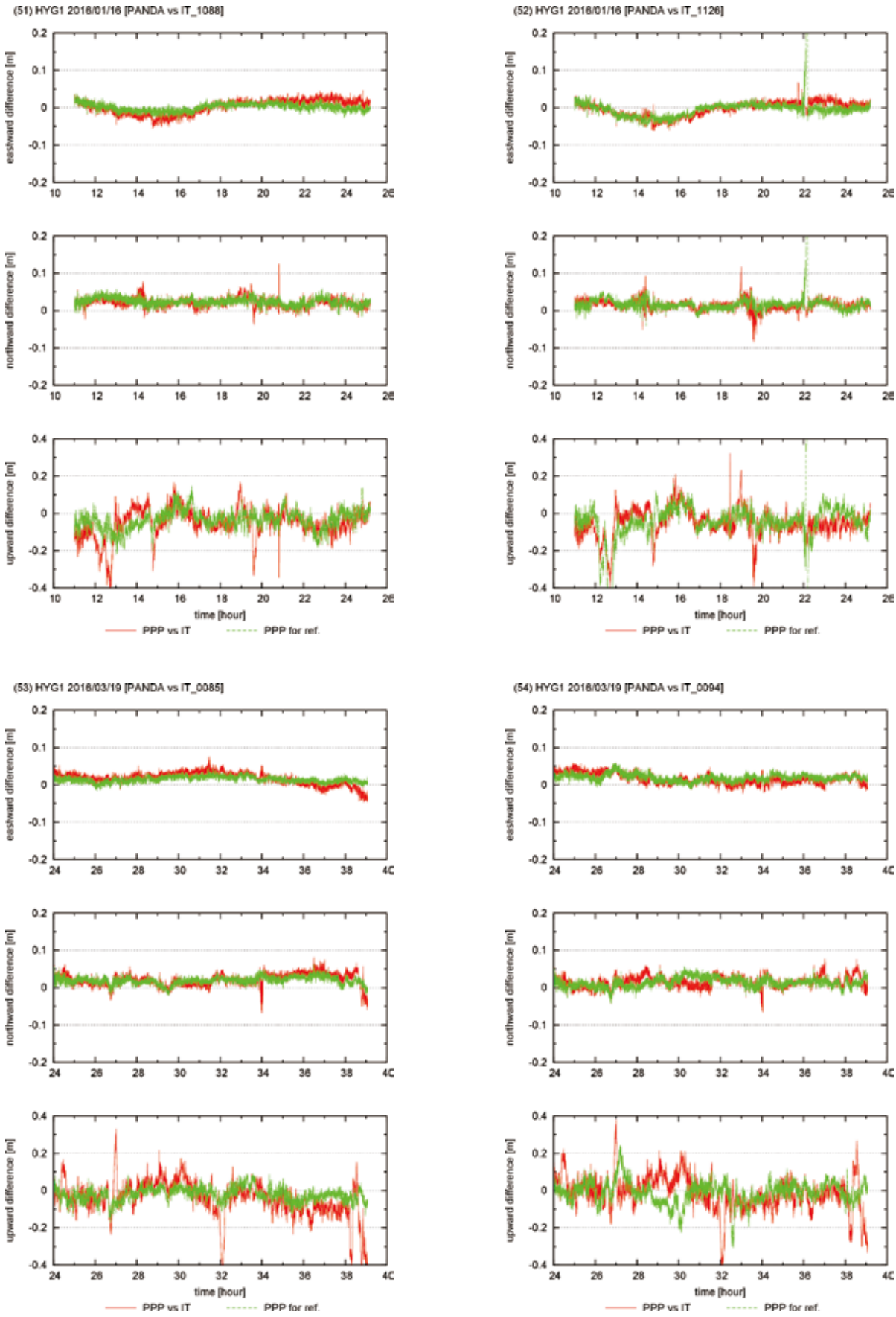

Fig. 5. （continued）
図 5.（続き）

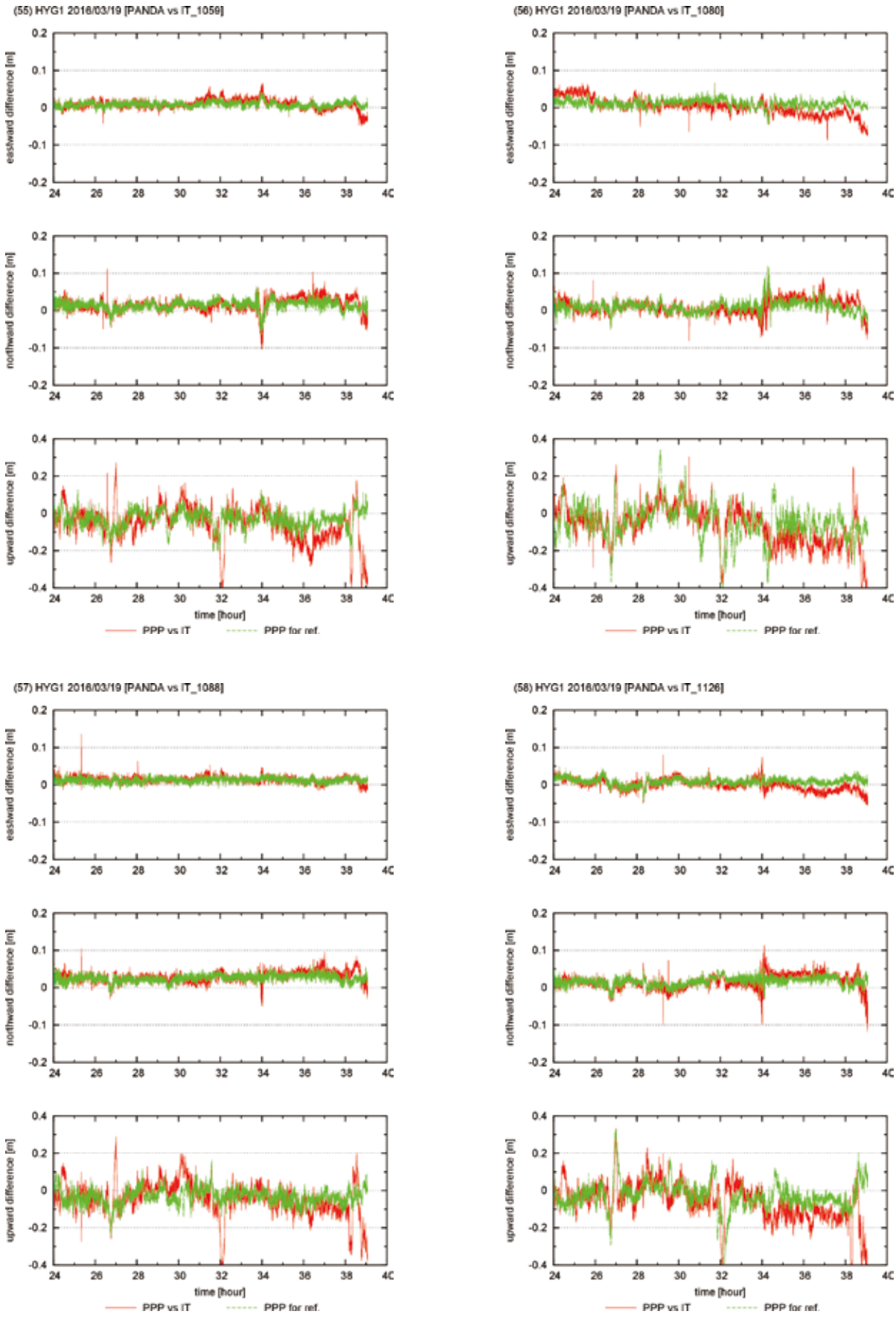

Fig. 5. （continued）
図 5.（続き）

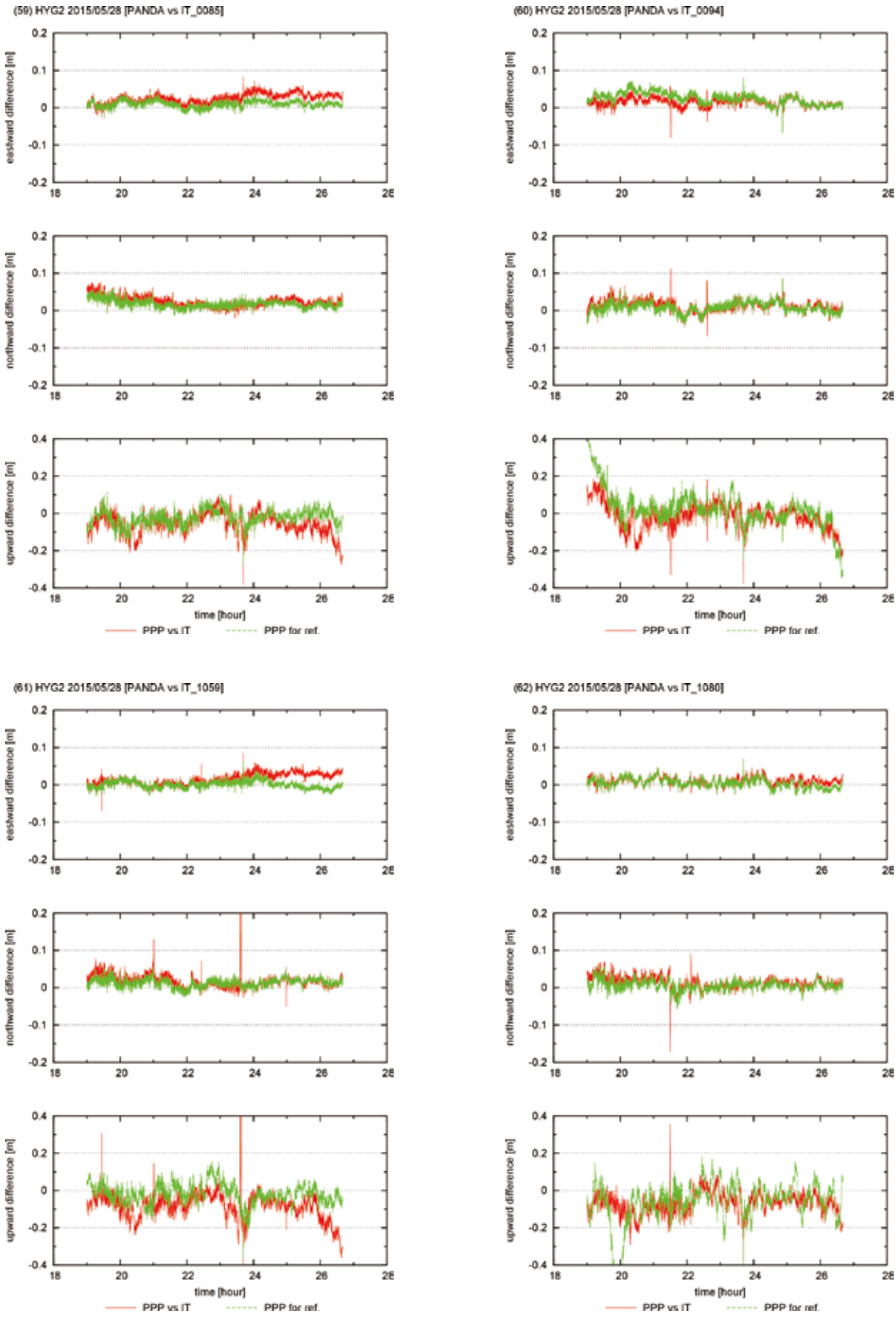

Fig. 5. （continued）
図 5.（続き）

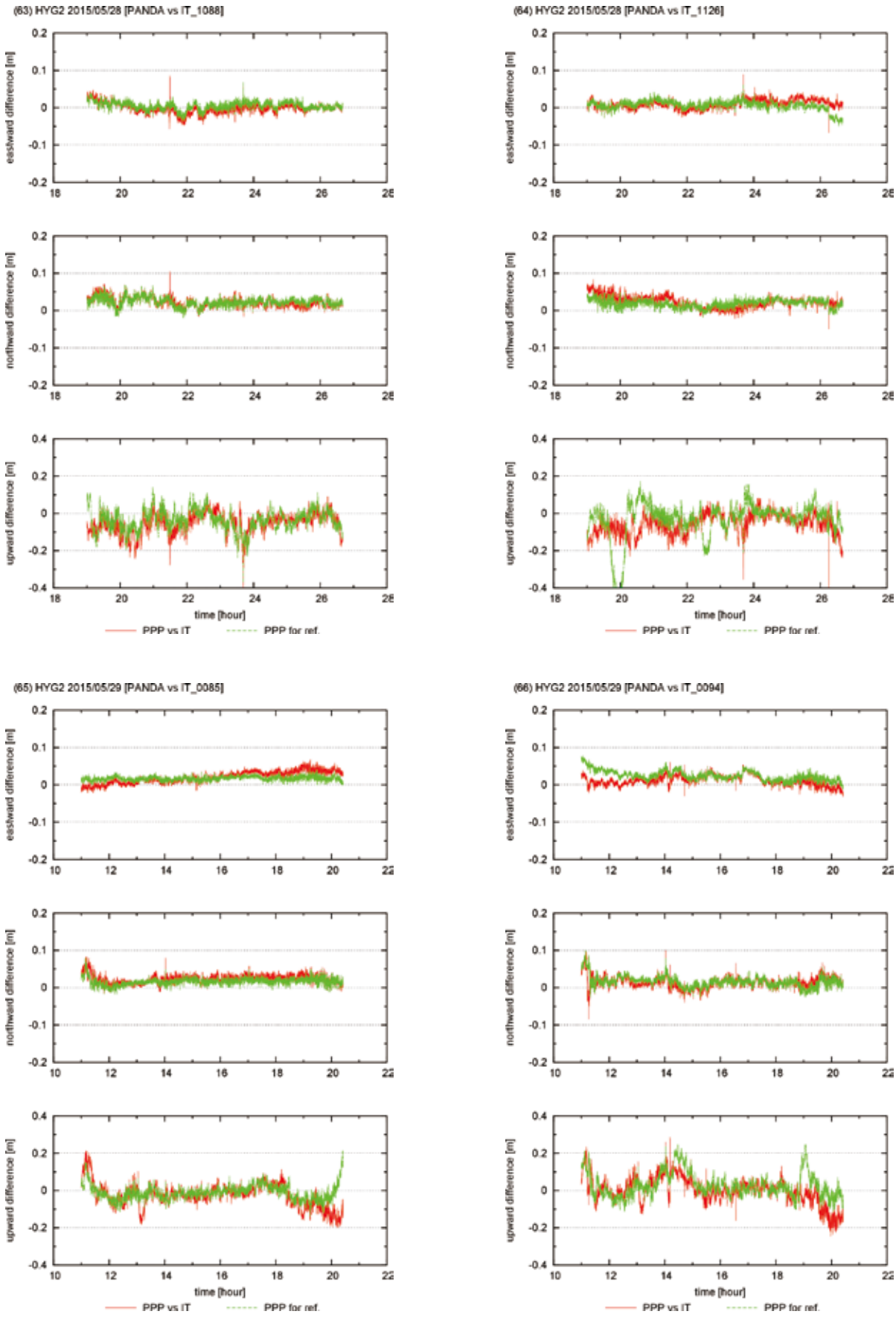

Fig. 5. （continued）
図 5.（続き）

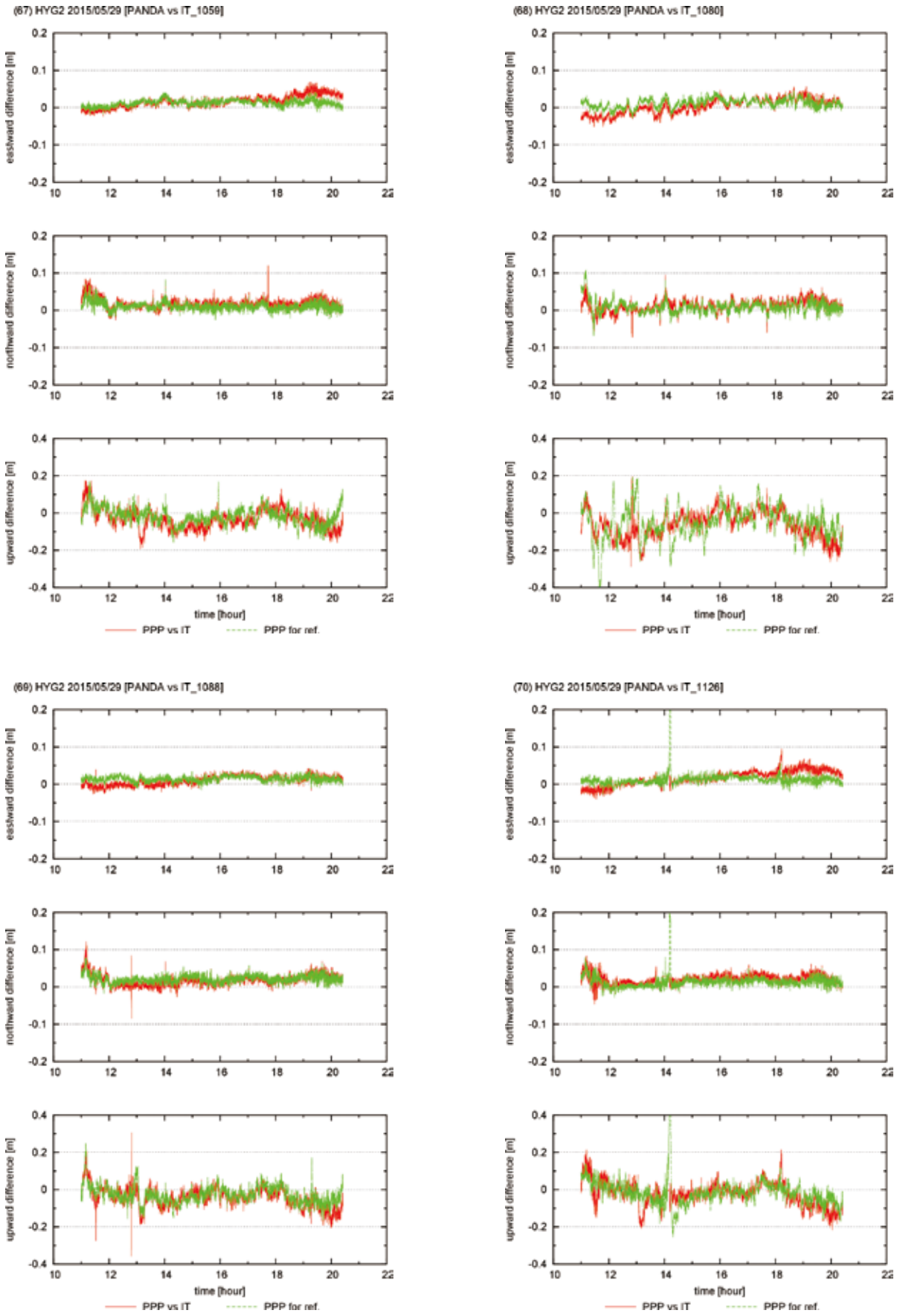

Fig. 5. （continued）
図 5.（続き）

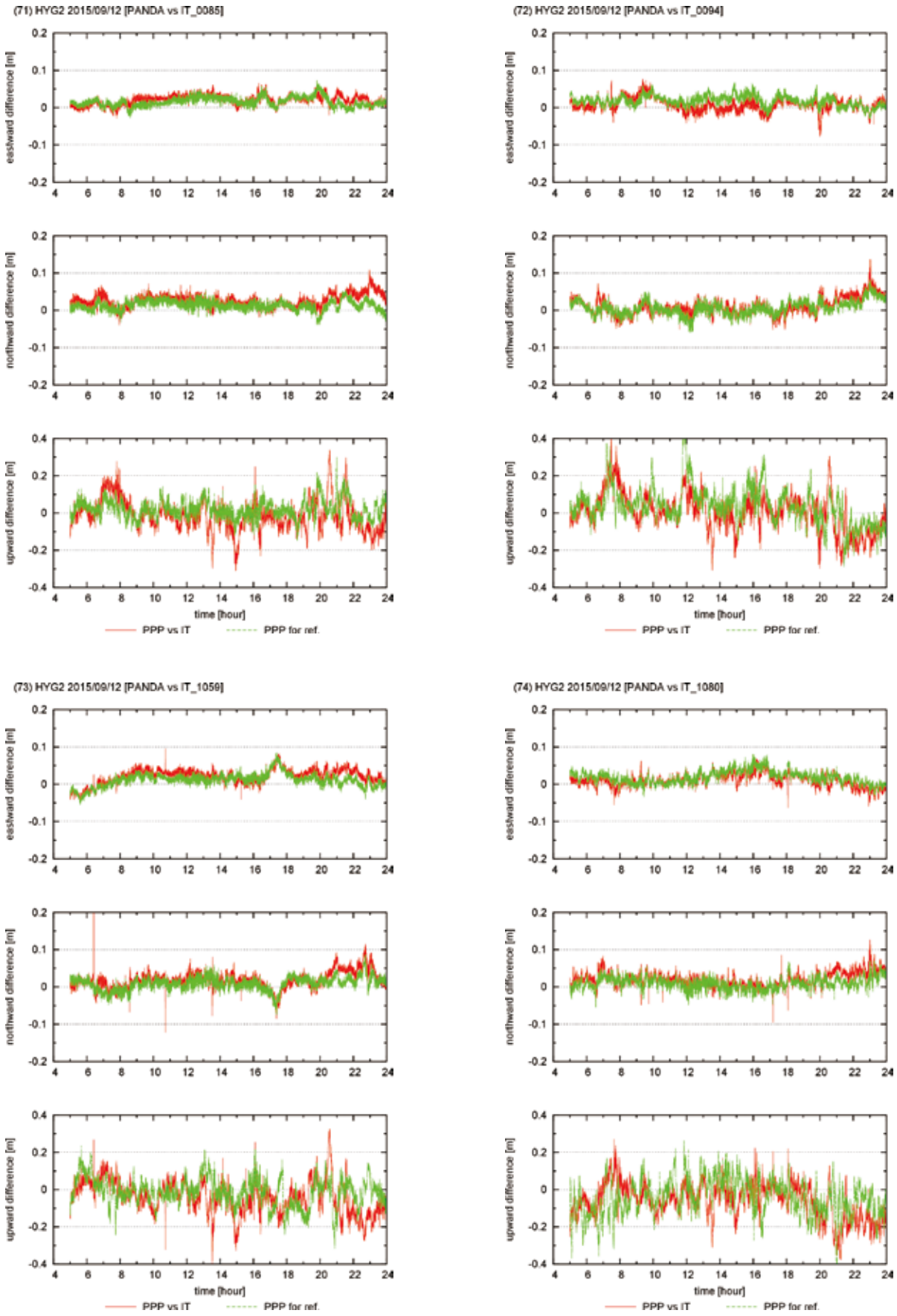

Fig. 5. （continued）
図 5.（続き）

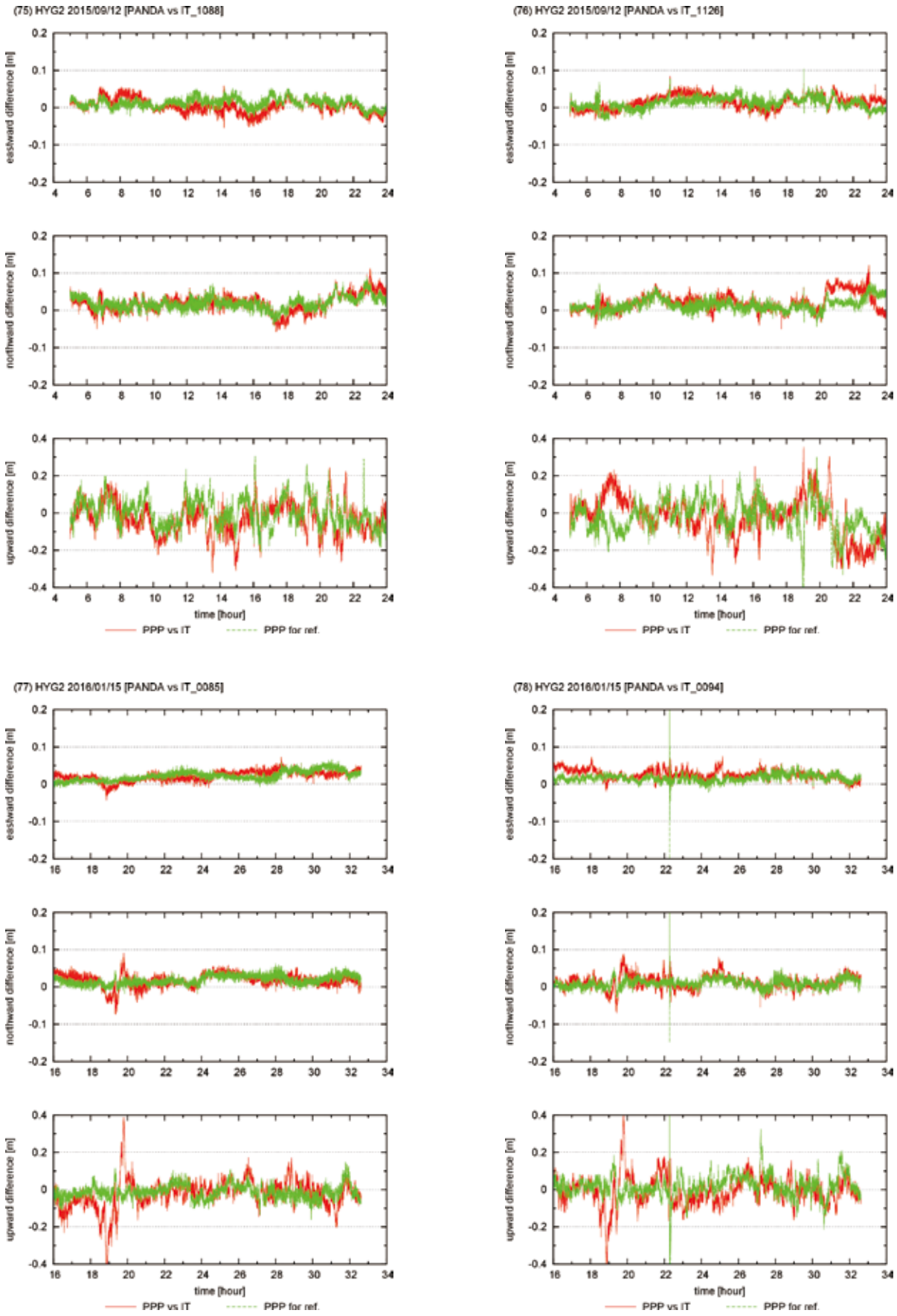

Fig. 5. （continued）
図 5.（続き）

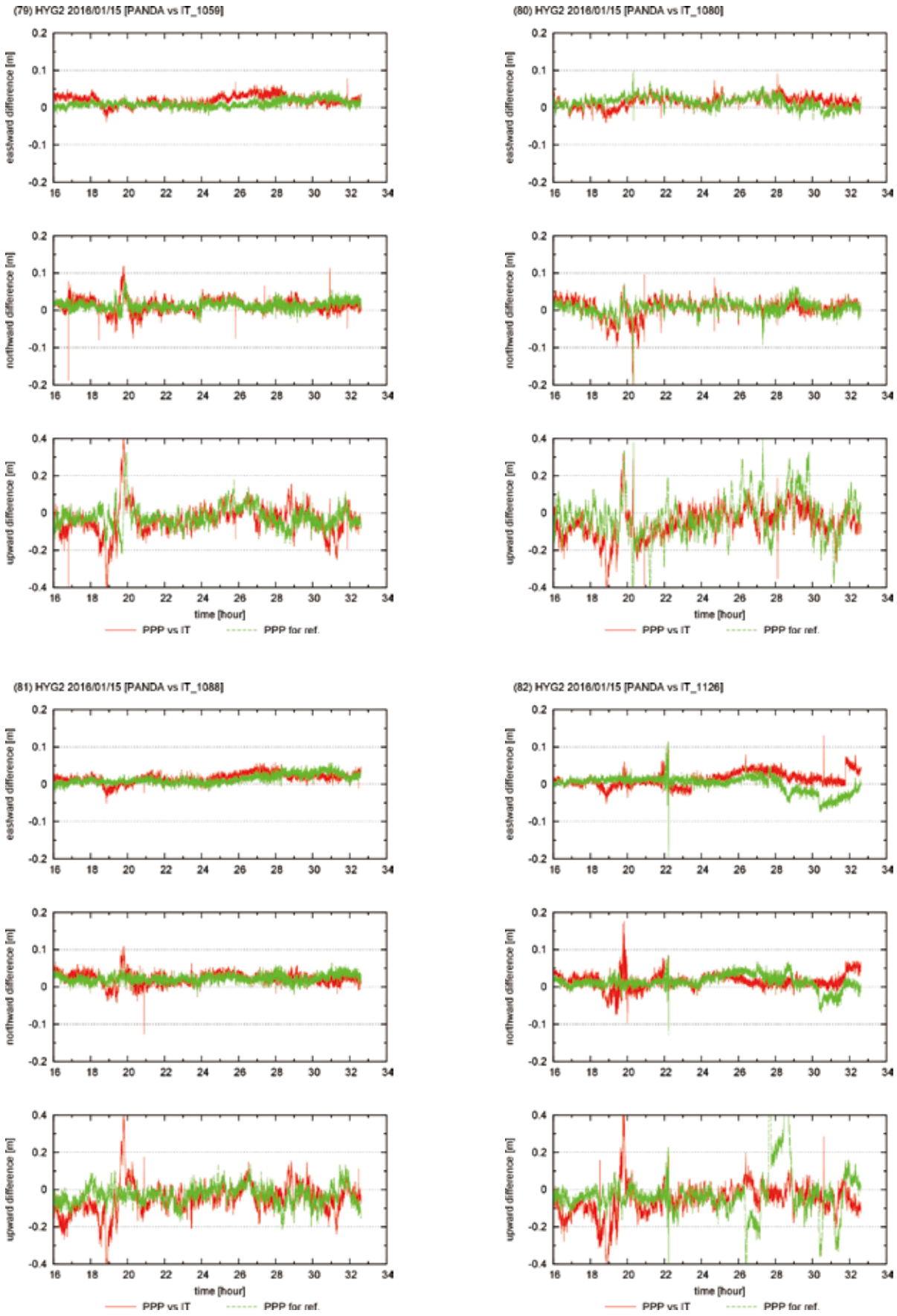

Fig. 5. （continued）
図 5.（続き）

Table 3. Values of average and standard deviation of the position differences. The names of the reference site for IT are shown as IT_[site name].

表 3. 各解析で得られた移動体位置の偏差の平均および標準偏差.

(a) TU12_2015/04/27

			Average (Bias)			Standard deviation		
			E-ward [m]	N-ward [m]	U-ward [m]	E-ward [m]	N-ward [m]	U-ward [m]
PANDA	vs	RTLKIB	-0.0030	0.0014	-0.0125	0.0128	0.0107	0.0380
PANDA	vs	IT_0036	0.0185	0.0198	0.0164	0.0113	0.0109	0.0428
PANDA	vs	IT_0037	0.0115	0.0027	0.0060	0.0087	0.0107	0.0416
PANDA	vs	IT_0172	0.0015	0.0173	-0.0186	0.0098	0.0131	0.0469
PANDA	vs	IT_0175	-0.0069	0.0144	0.0196	0.0465	0.0667	0.2895
PANDA	vs	IT_0179	0.0032	0.0146	-0.0127	0.0168	0.0153	0.0543
PANDA	vs	IT_0549	0.0107	0.0050	-0.0515	0.0104	0.0159	0.0617
PANDA	vs	IT_0550	0.0114	0.0084	-0.0089	0.0107	0.0136	0.0460
PANDA	vs	IT_0918	0.0098	0.0065	-0.0221	0.0074	0.0115	0.0412

(b) TU12_2015/08/07

			Average (Bias)			Standard deviation		
			E-ward [m]	N-ward [m]	U-ward [m]	E-ward [m]	N-ward [m]	U-ward [m]
PANDA	vs	RTLKIB	-0.0062	0.0035	0.0022	0.0138	0.0131	0.0734
PANDA	vs	IT_0036	0.0036	0.0231	-0.0040	0.0335	0.0255	0.0816
PANDA	vs	IT_0037	-0.0068	0.0071	-0.0127	0.0346	0.0249	0.0880
PANDA	vs	IT_0172	-0.0132	0.0308	-0.0543	0.0183	0.0219	0.0796
PANDA	vs	IT_0175	-0.0119	0.0201	-0.0384	0.0240	0.0226	0.0848
PANDA	vs	IT_0179	-0.0226	0.0126	-0.0228	0.0354	0.0304	0.0996
PANDA	vs	IT_0549	-0.0237	0.0061	-0.0288	0.0251	0.0252	0.0940
PANDA	vs	IT_0918	-0.0020	0.0117	-0.0386	0.0273	0.0231	0.0799

(c) TU12_2015/10/23

			Average (Bias)			Standard deviation		
			E-ward [m]	N-ward [m]	U-ward [m]	E-ward [m]	N-ward [m]	U-ward [m]
PANDA	vs	RTLKIB	-0.0028	0.0026	-0.0210	0.0157	0.0134	0.0491
PANDA	vs	IT_0036	0.0111	0.0201	0.0037	0.0116	0.0147	0.0693
PANDA	vs	IT_0037	0.0103	0.0067	-0.0043	0.0090	0.0140	0.0638
PANDA	vs	IT_0172	0.0024	0.0198	-0.0400	0.0115	0.0127	0.0581
PANDA	vs	IT_0175	0.0067	0.0164	-0.0356	0.0101	0.0116	0.0544
PANDA	vs	IT_0179	0.0039	0.0139	-0.0079	0.0138	0.0168	0.0585
PANDA	vs	IT_0549	-0.0032	0.0094	-0.0416	0.0159	0.0144	0.0697
PANDA	vs	IT_0550	0.0075	0.0092	-0.0214	0.0104	0.0113	0.0542
PANDA	vs	IT_0918	0.0076	0.0091	-0.0369	0.0107	0.0133	0.0624

(d) SAGA_2012/11/24

			Average (Bias)			Standard deviation		
			E-ward [m]	N-ward [m]	U-ward [m]	E-ward [m]	N-ward [m]	U-ward [m]
PANDA	vs	RTLKIB	0.0052	0.0000	-0.0020	0.0093	0.0066	0.0289
PANDA	vs	IT_0759	0.0104	0.0126	-0.0519	0.0173	0.0124	0.0584
PANDA	vs	IT_3047	0.0187	0.0026	-0.0139	0.0161	0.0160	0.0407
PANDA	vs	IT_3048	0.0142	0.0102	-0.0274	0.0077	0.0096	0.0382
PANDA	vs	IT_3051	0.0143	0.0140	-0.0057	0.0084	0.0101	0.0299
PANDA	vs	IT_5105	0.0113	0.0138	-0.0319	0.0095	0.0107	0.0417

Table 3. （continued）
表 3.（続き）

(e) HYG1_2015/05/29

			Average (Bias)			Standard deviation		
			E-ward [m]	N-ward [m]	U-ward [m]	E-ward [m]	N-ward [m]	U-ward [m]
PANDA	vs	RTLKIB	0.0019	-0.0011	-0.0224	0.0117	0.0110	0.0924
PANDA	vs	IT_0085	0.0179	0.0165	-0.0448	0.0104	0.0114	0.0939
PANDA	vs	IT_0094	0.0057	0.0079	-0.0250	0.0239	0.0238	0.1208
PANDA	vs	IT_1059	0.0158	0.0100	-0.0702	0.0112	0.0136	0.0939
PANDA	vs	IT_1080	-0.0013	0.0148	-0.0771	0.0124	0.0170	0.0897
PANDA	vs	IT_1088	0.0029	0.0161	-0.0643	0.0178	0.0190	0.0959
PANDA	vs	IT_1126	0.0075	0.0151	-0.0453	0.0129	0.0123	0.0985

(f) HYG1_2015/09/11

			Average (Bias)			Standard deviation		
			E-ward [m]	N-ward [m]	U-ward [m]	E-ward [m]	N-ward [m]	U-ward [m]
PANDA	vs	RTLKIB	0.0012	0.0032	-0.0026	0.0110	0.0085	0.0579
PANDA	vs	IT_0085	0.0218	0.0155	-0.0176	0.0099	0.0116	0.0608
PANDA	vs	IT_0094	0.0128	0.0068	0.0032	0.0207	0.0159	0.0614
PANDA	vs	IT_1059	0.0137	0.0139	-0.0572	0.0147	0.0138	0.0539
PANDA	vs	IT_1080	0.0074	0.0147	-0.0610	0.0117	0.0146	0.0664
PANDA	vs	IT_1088	0.0140	0.0136	-0.0348	0.0102	0.0119	0.0539
PANDA	vs	IT_1126	0.0153	0.0151	-0.0186	0.0123	0.0130	0.0658

(g) HYG1_2015/12/12

			Average (Bias)			Standard deviation		
			E-ward [m]	N-ward [m]	U-ward [m]	E-ward [m]	N-ward [m]	U-ward [m]
PANDA	vs	RTLKIB	0.0020	0.0016	-0.0151	0.0142	0.0089	0.0480
PANDA	vs	IT_0085	0.0183	0.0205	-0.0182	0.0098	0.0105	0.0624
PANDA	vs	IT_0094	0.0180	0.0106	0.0328	0.0146	0.0144	0.1277
PANDA	vs	IT_1059	0.0160	0.0166	-0.0307	0.0180	0.0159	0.0808
PANDA	vs	IT_1080	0.0164	0.0077	0.0128	0.0164	0.0189	0.0678
PANDA	vs	IT_1088	0.0144	0.0250	-0.0300	0.0086	0.0124	0.0598
PANDA	vs	IT_1126	0.0102	0.0203	-0.0383	0.0101	0.0112	0.0596

(h) HYG1_2016/01/16

			Average (Bias)			Standard deviation		
			E-ward [m]	N-ward [m]	U-ward [m]	E-ward [m]	N-ward [m]	U-ward [m]
PANDA	vs	RTLKIB	-0.0102	-0.0026	0.0178	0.0080	0.0169	0.0746
PANDA	vs	IT_0085	0.0030	0.0158	-0.0361	0.0193	0.0108	0.0820
PANDA	vs	IT_0094	0.0121	0.0092	-0.0255	0.0212	0.0165	0.1038
PANDA	vs	IT_1059	-0.0010	0.0128	-0.0480	0.0210	0.0147	0.0813
PANDA	vs	IT_1080	0.0237	0.0044	-0.0662	0.0468	0.0185	0.1032
PANDA	vs	IT_1088	0.0026	0.0219	-0.0521	0.0184	0.0115	0.0790
PANDA	vs	IT_1126	-0.0033	0.0142	-0.0497	0.0187	0.0124	0.0747

Table 3. （continued）
表 3.（続き）

(l) HYG1_2016/03/19

			Average (Bias)			Standard deviation		
			E-ward [m]	N-ward [m]	U-ward [m]	E-ward [m]	N-ward [m]	U-ward [m]
PANDA	vs	RTLKIB	-0.0049	0.0005	0.0027	0.0185	0.0152	0.0995
PANDA	vs	IT_0085	0.0170	0.0211	-0.0423	0.0161	0.0157	0.0958
PANDA	vs	IT_0094	0.0164	0.0149	-0.0116	0.0137	0.0142	0.0907
PANDA	vs	IT_1059	0.0093	0.0163	-0.0542	0.0123	0.0170	0.0931
PANDA	vs	IT_1080	0.0031	0.0108	-0.0627	0.0218	0.0193	0.1054
PANDA	vs	IT_1088	0.0136	0.0288	-0.0433	0.0082	0.0134	0.0899
PANDA	vs	IT_1126	0.0004	0.0164	-0.0561	0.0143	0.0177	0.1007

(j) HYG2_2015/05/28

			Average (Bias)			Standard deviation		
			E-ward [m]	N-ward [m]	U-ward [m]	E-ward [m]	N-ward [m]	U-ward [m]
PANDA	vs	RTLKIB	-0.0016	0.0033	-0.0057	0.0097	0.0101	0.0452
PANDA	vs	IT_0085	0.0250	0.0239	-0.0550	0.0131	0.0134	0.0569
PANDA	vs	IT_0094	0.0149	0.0122	-0.0170	0.0114	0.0146	0.0686
PANDA	vs	IT_1059	0.0156	0.0169	-0.0830	0.0148	0.0158	0.0716
PANDA	vs	IT_1080	0.0099	0.0136	-0.0689	0.0106	0.0155	0.0556
PANDA	vs	IT_1088	-0.0015	0.0224	-0.0522	0.0135	0.0126	0.0545
PANDA	vs	IT_1126	0.0101	0.0231	-0.0560	0.0114	0.0151	0.0531

(k) HYG2_2015/05/29

			Average (Bias)			Standard deviation		
			E-ward [m]	N-ward [m]	U-ward [m]	E-ward [m]	N-ward [m]	U-ward [m]
PANDA	vs	RTLKIB	0.0054	0.0007	-0.0054	0.0114	0.0117	0.0549
PANDA	vs	IT_0085	0.0203	0.0229	-0.0243	0.0156	0.0116	0.0617
PANDA	vs	IT_0094	0.0115	0.0137	0.0013	0.0130	0.0148	0.0693
PANDA	vs	IT_1059	0.0172	0.0170	-0.0308	0.0155	0.0125	0.0533
PANDA	vs	IT_1080	0.0036	0.0118	-0.0619	0.0196	0.0159	0.0705
PANDA	vs	IT_1088	0.0099	0.0181	-0.0405	0.0120	0.0143	0.0522
PANDA	vs	IT_1126	0.0174	0.0199	-0.0217	0.0192	0.0123	0.0634

(l) HYG2_2015/09/12

			Average (Bias)			Standard deviation		
			E-ward [m]	N-ward [m]	U-ward [m]	E-ward [m]	N-ward [m]	U-ward [m]
PANDA	vs	RTLKIB	-0.0044	-0.0041	-0.0056	0.0207	0.0232	0.0896
PANDA	vs	IT_0085	0.0200	0.0256	-0.0113	0.0127	0.0166	0.0810
PANDA	vs	IT_0094	0.0084	0.0104	0.0050	0.0172	0.0222	0.0990
PANDA	vs	IT_1059	0.0210	0.0174	-0.0394	0.0195	0.0224	0.0867
PANDA	vs	IT_1080	0.0106	0.0195	-0.0609	0.0171	0.0195	0.0924
PANDA	vs	IT_1088	0.0045	0.0187	-0.0299	0.0179	0.0226	0.0793
PANDA	vs	IT_1126	0.0155	0.0214	-0.0221	0.0172	0.0226	0.1080

Table 3. (continued)
表 3. (続き)

(m) HYG2_2016/01/15

			Average (Bias)			Standard deviation		
			E-ward [m]	N-ward [m]	U-ward [m]	E-ward [m]	N-ward [m]	U-ward [m]
PANDA	vs	RTLKIB	0.0132	-0.0006	-0.0166	0.0162	0.0141	0.0836
PANDA	vs	IT_0085	0.0218	0.0180	-0.0241	0.0131	0.0165	0.0790
PANDA	vs	IT_0094	0.0257	0.0120	-0.0072	0.0130	0.0176	0.0786
PANDA	vs	IT_1059	0.0194	0.0133	-0.0361	0.0129	0.0166	0.0793
PANDA	vs	IT_1080	0.0162	0.0056	-0.0525	0.0142	0.0242	0.0848
PANDA	vs	IT_1088	0.0161	0.0223	-0.0493	0.0129	0.0150	0.0841
PANDA	vs	IT_1126	0.0139	0.0157	-0.0563	0.0183	0.0190	0.0849

(n) SIO buoy_2011/03/14

			Average (Bias)			Standard deviation		
			E-ward [m]	N-ward [m]	U-ward [m]	E-ward [m]	N-ward [m]	U-ward [m]
GIPSY	vs	PANDA	0.0014	0.0038	0.0167	0.0042	0.0063	0.0227
GIPSY	vs	RTKLIB	-0.0088	0.0093	0.0077	0.0223	0.0150	0.0499

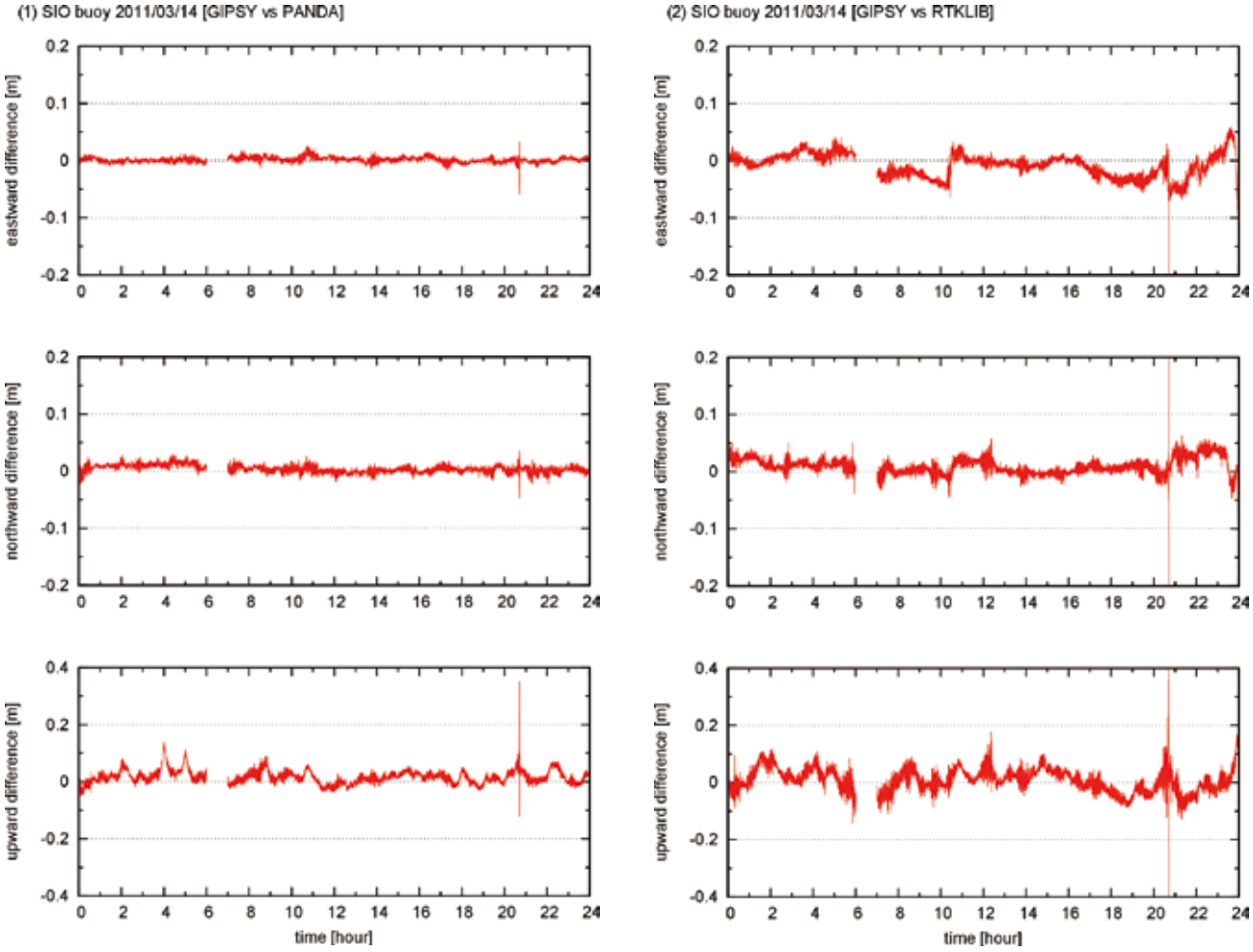

Fig. 6. Time series of position differences of the SIO buoy between the results by (1) GIPSY and PANDA, and (2) GIPSY and RTKLIB in the local ENU coordinates. The eastern, northern, and vertical components are displayed on the top, middle, and bottom panels, respectively.

図 6. (1) GIPSY と PANDA, (2) GIPSY と RTKLIB との比較からそれぞれ得られた，SIO ブイ位置解の偏差の時系列．偏差はローカル ENU 座標系を用いて，上からそれぞれ東向き，北向き，上向きの成分を示す．

Considering the results from all the data sets analyzed here, the PANDA PPP software with ambiguity resolution (PPP-AR) is a good candidate for positioning the ship as part of the GPS-A analysis. It provided more stable solution even in situations with loss of data, perhaps due to solving the integer ambiguity, which we did not for RTKLIB. It is noted for the differential positioning, which is a method to reduce the error using the reference station, that the long-term biases of the reference positions also propagate directly to the rover's solution.

For the purpose of GPS-A observation, where one solves the static positions using acoustic ranging data from the estimated ship track with the period of about 10–20 hours (instead of using the electromagnetic wave from the satellites with estimated orbits for GNSS), long-term variation would decrease the precision of the seafloor positioning rather than short-term perturbation. Because JCG uses IT to estimate the ship track for the routine analysis of the GPS-A, the biases of 1–3 cm from the PPP (i.e., from the global geodetic reference frame) would affect their results. The horizontal biases of terrestrial sites also varied in a range of about 1 cm with the campaign and the selection of the reference, which results in the long-term uncertainty of the ship track estimation. Although it is smaller than the GPS-A horizontal error of 2–3 cm which is considered to be mainly caused by the temporal and spatial variations of the acoustic velocity (e.g., Sato et al., 2013), it is possible that the stability of the time series of the seafloor positioning may improve when using the PPP results. In any case, because the true positions of rover are unavailable, we need to solve the seafloor benchmark positions and compare its long-term stability to validate the PPP solutions for the GPS-A observation. In addition, we should continue this study to evaluate the accuracy of the near real-time GPS-A analysis using PPP, in which one can obtain the GPS-A solution during the observation cruise.

Acknowledgements

The ship-borne GNSS data were collected by the Hydrographic and Oceanographic Department of Japan Coast Guard during their GPS-A campaign observations. The terrestrial GNSS data and its daily positions for the differential positioning were provided by the Geospatial Information Authority of Japan. The GNSS data of the SIO buoy and its PPP solution using GIPSY were provided by C. D. Chadwell of the Scripps Institution of Oceanography. The GNSS software IT was provided by O. L. Colombo of the NASA Goddard Space Flight Center. RTKLIB is an open source software developed by T. Takasu of the Tokyo University of Marine Science and Technology (available at http://www.rtklib.com/). The first author processed the data using PANDA in modified version at the Scripps Orbit and Permanent Array Center, with the support of D. Goldberg. Comments from an anonymous reviewer have improved the paper substantially. Some figures were produced with the GMT software (Wessel and Smith, 1991). This study was done during the first author's visit at the Scripps Institution of Oceanography, University of California, San Diego under the support of the Ministry of Education, Culture, Sports, Science and Technology in Japan.

References

Bertiger W., S. D. Desai, B. Haines, N. Harvey, A.W. Moore, S. Owen, and J.P. Weiss (2010) Single receiver phase ambiguity resolution with GPS data, J. Geod., 84, 327–337.

Colombo, O. L. (1998) Long-Distance Kinematic GPS, in GPS for Geodesy 2nd Edition, edited

by P. J. E. Teunissen and A. Kleusberg, Springer, 537–568.

Fujita, M., T. Ishikawa, M. Mochizuki, M. Sato, S. Toyama, M. Katayama, Y. Matsumoto, T. Yabuki, A. Asada, and O. L. Colombo (2006) GPS/Acoustic seafloor geodetic observation: Method of data analysis and its application, Earth Planets Space, 58, 265–275.

Fujita, M. and T. Yabuki (2003) A Way of Accuracy Estimation of K-GPS Results in the Seafloor Geodetic Measurement, Tech. Bull. on Hydrogr. Oceanogr., 21, 62–66 (in Japanese).

Ge, M., G. Gendt, M. Rothacher, C. Shi, and J. Liu (2008) Resolution of GPS carrier-phase ambiguities in precise point positioning (PPP) with daily observations, J. Geod., 82 (7), 389–399.

Geng, J., F. N. Teferle, C. Shi, X. Meng, A. H. Dodson, and J. Liu (2009) Ambiguity resolution in precise point positioning with hourly data, GPS Solut., 13, 263–270, doi:10.1007/s10291–009–0119–2.

Geng, J., F. N. Teferle, X. Meng, and A. H. Dodson (2010) Kinematic precise point positioning at remote marine platforms, GPS Solut., 14, 343–350, doi:10.1007/s10291–009–0157–9.

Geng, J., Y. Bock, D. Melgar, B.W. Crowell, and J.S. Haase (2013) A new seismogeodetic approach applied to GPS and accelerometer observations of the 2012 Brawley seismic swarm: Implications for earthquake early warning, Geochem. Geophys. Geosyst., 14, 2124–2142.

Kawai, K., M. Fujita, T. Ishikawa, Y. Matsumoto, and M. Mochizuki (2006) Accuracy evaluation of the long baseline KGPS, Tech. Bull. on Hydrogr. Oceanogr., 24, 80–88 (in Japanese).

Melgar D. and Y. Bock (2015) Kinematic earthquake source inversion and tsunami runup prediction with regional geophysical data, J. Geophys. Res., 120 3324–3349.

Nakagawa, H., T. Toyofuku, K. Kotani, B. Miyahara, C. Iwashita, S. Kawamoto, Y. Hatanaka, H. Munekane, M. Ishimoto, T. Yutsudo, N. Ishikura, and Y. Sugawara (2009) Development and validation of GEONET new analysis strategy (Version 4). J. Geographical Survey Inst., 118, 1–8 (in Japanese).

Saito, H., Y. Seki, N. Umehara, T. Asakura, and M. Sato (2010) Effectiveness of rapid orbit in KGPS analysis of seafloor geodetic observation, Rep. of Hydrogr. Oceanogr. Res., 46, 32–38 (in Japanese).

Sato, M., M. Fujita, Y. Matsumoto, H. Saito, T. Ishikawa, and T. Asakura (2013) Improvement of GPS/acoustic seafloor positioning precision through controlling the ship's track line, J. Geod., 87, 825–842, doi:10.1007/s00190–013–0649–9.

Shi, C., Q. Zhao, J. Geng, Y. Lou, M. Ge, and J. Liu (2008) Recent development of PANDA software in GNSS data processing. in Proceedings of the society of photographic instrumentation engineers, 7285, 72851S. doi:10.1117/12.816261.

Wessel, P. and W. H. F. Smith (1991), Free software helps map and display data, Eos. Trans. AGU, 72, 441, doi:10.1029/90EO00319.

海上観測機器に対する精密単独測位と基線解析の長期安定性評価

渡邉俊一，Yehuda BOCK,
C. David CHADWELL, Peng FANG,
Jianghui GENG

要　旨

精密単独測位（PPP）は，ローカルな陸上基準点に依存しないため，GPS-A 観測で必要とされる，

外洋域における精密船位推定において有用なツールとなることが期待される．本研究では，同観測で得られた 1 Hz GNSS データについて，異なるソフトウェアによる解析を実施し，その長期的な安定性を調査した．その結果，基準点における摂動にも影響される基線解析に比べて，PPP は安定した解を与えることがわかった．さらに，整数値バイアス（ambiguity）を解決した PPP は, データの欠損に対してもロバストであることも示された.